12-2016

Mathematical analysis of feedback targets of BMP signaling in Drosophila embryonic development

Yan Luo
Purdue University

Graduate School Form
30 Updated 12/26/2015

PURDUE UNIVERSITY
GRADUATE SCHOOL
Thesis/Dissertation Acceptance

This is to certify that the thesis/dissertation prepared

By Yan Luo

Entitled
Mathematical Analysis of Feedback Targets of BMP Signaling in Drosophila Embryonic Development

For the degree of Master of Science in Agricultural and Biological Engineering

Is approved by the final examining committee:

David M. Umulis
Co-chair

Tamara L. Kinzer-Ursem
Co-chair

Taeyoon Kim

To the best of my knowledge and as understood by the student in the Thesis/Dissertation Agreement, Publication Delay, and Certification Disclaimer (Graduate School Form 32), this thesis/dissertation adheres to the provisions of Purdue University's "Policy of Integrity in Research" and the use of copyright material.

Approved by Major Professor(s): David M. Umulis, Tamara L. Kinzer-Ursem

Approved by: Bernard A. Engel 08/19/2016

Head of the Departmental Graduate Program Date

MATHEMATICAL ANALYSIS OF FEEDBACK TARGETS OF BMP SIGNALING IN DROSOPHILA EMBRYONIC DEVELOPMENT

A Dissertation

Submitted to the Faculty

of

Purdue University

by

Yan Luo

In Partial Fulfillment of the

Requirements for the Degree

of

Master of Science in Agricultural and Biological Engineering

December 2016

Purdue University

West Lafayette, Indiana

This thesis is dedicated to my parents. Thanks for loving me all the time. I miss you so much, Dad.

ACKNOWLEDGMENTS

I would like to thank my two co-advisors, Dr. David M. Umulis and Dr. Tamara L. Kinzer-Ursem, for their valuable time they spent on guiding me. In addition, I would like to thank them for their patience and support when I was having the hardest time of my life. Thank you Dr. Taeyoon Kim for agreeing to serve on my committee and providing suggestions and comments.

I am also grateful to my wonderful lab-mates Yan Huang, Md. Shahriar Karim, Linlin Li, Tze-Ching Wu, Xu Wang, Ye Bu, Matthew Thompson, Bobby Madamanchi, Nimisha Bajaj, Joyatee Sarker, Thembi Mdluli, and Kinzer-Urserm lab members Matthew Pharris, Katherine Clayton, Mrugesh Krishna Parasa, Janelle Weslyn Salameh, Scott Bolton, Aya Saleh, Julia Fraseur and Andrew Witten for their collaboration and help.

Special thanks goes to former PULSe coordinator Emily Bramson, I hope you enjoy your life after retirement. I am also grateful to Dr. Charles Babbs. In addition I would like to extend my thanks to all my friends in Purdue and back in China.

Finally I would like to thank my girlfriend Yina, who has always been the source of great peace and happiness of my life.

TABLE OF CONTENTS

Page

LIST OF TABLES vi

LIST OF FIGURES vii

ABSTRACT x

1 Introduction 1

2 Background 5

2.1 Development of *Drosophila* 5

2.2 Morphogenesis and Morphogen 8

2.2.1 Reaction-Diffusion and Positional Information 8

2.2.2 BMP in *Drosophila* Embryonic Development 13

2.3 Mathematical Models of BMP in *Drosophila* Embryo 17

3 Problem Description 21

3.1 Regulation of Crossveinless 2 22

3.2 Eiger Promoting BMP Signal 23

4 Methods 25

4.1 Local Model 25

4.2 Bistability Analysis 28

4.3 One-Dimensional Spatial Model 30

4.3.1 Finite Difference Scheme 32

4.3.2 Proposed Mechanisms 33

4.4 Data Collection 35

4.5 Pareto Frontier 35

5 Results and Discussion 39

5.1 Local Model and Bistability Analysis 39

5.2 1D Spatial Model and Bistability 43

Page

5.3 Data Collection and Processing 47
5.4 Model Comparison 51
6 conclusion and future work 57
LIST OF REFERENCES 61

LIST OF TABLES

Table Page

5.1 Table of data used and source 48

LIST OF FIGURES

Figure Page

2.1 Life cycle of *Drosophila melanogaster*: Fertilized egg goes to blastoderm and gastrulation stages after cleavage, then it becomes larva. After larva development and metamorphosis, it becomes an adult fly and restarts this cycle.(Image adapted from [29] with permission) 6

2.2 Early stages of embryonic development: Stage 1: newly laid egg, pronuclear fusion; Stage 2: pre-blastoderm, early cell division, and start of cleavage; Stage 3: pole-cell formation; Stage 4: syncytial blastoderm and end of cleavage divisions; Stage 5: cellularization of the cellular blastoderm. (Image adapted from [30] with permission) 7

2.3 Illustration of activator-inhibitor pair RD system. i) A random concentration fluctuation cause some cells have higher concentration of activator(green line), and a peak of activator is formed because of its autoactivation; ii) Since the activator can also promote inhibitor production, a rise of inhibitor concentration happens; iii) With faster diffusion of inhibitor, so at the peak, the inhibitor is not enough to prevent the formation of a stabilized peak from the positive feedback loop, and away from the peak, inhibitor repress production of activator; iv) Further away from the repressed region, new peaks form; v) With similar process, a spatial-periodic pattern of activator and inhibitor is formed.(Image adapted from [32] with permission) 9

2.4 a)Diagram of the BMP-Sox9-Wnt network. b) Left: simulation result (Sox9 distribution) based on the RD system of the network, with different perturbations. Right: Experimental results of mouse limb buds in Sox9-EGFP images with same perturbations (Image adapted from [33] with permission). 10

2.5 French flag model in which two different threshold concentrations of a morphogen elicit three distinct responses. 12

2.6 The French Flag model explaining Bicoid mediated Anterior-Posterior patterning in *Drosophila* embryo.(Adapted from [34] with permission) . . . 13

Figure Page

2.7 a) Diagram of BMP signaling pathway in *Drosophila*, description in text (Image adapted from [44] with permission). b) Axes and geometry of a Drosophila blastoderm embryo(A: anterior, P: posterior, D: dorsal, V: ventral) (Image adapted from [45] with permission). c) Cross-section of a Drosophila embryo in the early stages of development showing the different regions of gene expression (Image adapted from [8] with permission). . 16

2.8 Workflow for the Development of a 3D whole embryo-scale model. Geometric information are coded into a 3D representation of the Drosophila embryo. Each model representing different proposed mechanisms are then simulated yielding the distribution of all proteins in the system. Models are trained from data extracted from pMad staining images of WT and 8 mutants. Differences between model output and image data are used to compare models quantitatively. (Image adapted from [8] with permission) 18

3.1 Diagram of interactions between Cv2, BMP and BMP receptors. BMP can bind both Type I receptor and Cv2 and there is an intermediating complex formed with BMP, Cv2 and Type I receptor.(Image adapted from [25] with permission) 23

3.2 pMad Staining of Eiger and Cv2 mutant embryos: (A I) dorsal view pMad staining images (A, D and G), mean intensities (B, E, and H), and variability (C, F, and I) of*egr* embryos (AC), 8 *cv-2* embryos (DF), 15 *egr cv-2* embryos (GI), the corresponding control group (wild type).(Image adapted from [26] with permission) 24

4.1 Diagram of Local Model 26

4.2 Set up parameter values for continuation analysis in MatCont 29

4.3 Diagram of Spatial Model 30

4.4 Diagrams of Major Alternative Networks: a) Eiger promoting phosphorylation/No BCR; b) Eiger promotes production of receptor/No BCR; c) Eiger inhibits dissociation of BR/No BCR; d) Eiger promoting phosphorylation/With BCR; e) Eiger promotes production of receptor/With BCR; f) Eiger inhibits dissociation of BR/With BCR 34

4.5 Example of Pareto Front, described in text (Image courtesy of Michael Pargett) 37

4.6 Left: Brute Force Method of generating Pareto Fronts; Right: an example of approximating Pareto frontier for a simple bi-objective problem . . . 38

5.1 Steady-state Curves of Local Model with different production rate of Eiger 42

Figure Page

5.2 BMP and pMad spatial distribution evolving with time: a) pMad distribution at different time points, circles on the steady state distribution are the pMad levels of cells ending on high or low states of the bistability curve; b) BMP distribution at same time points and cells of high and low pMad states are also showed as circles. 45

5.3 Evolution of pMad ending in two states: a) pMad concentration change with time; b) trace of BMP and pMad concentrations of two types of cells on the stability curve 46

5.4 pMad distribution at 60 min of WT and *eiger* heterozygous mutant. In heterozygous simulation, production rate of Eiger is half of the one used in wild type. 47

5.5 Procedures of data extraction from pMad staining images 49

5.6 An example (*egr* -/- mutant) of data calibration 50

5.7 a) An example of simulation result having good fitness of data. b) objective points and Pareto frontier of model BCR+ and BCR- 52

5.8 Pareto fronts of models with different Eiger functions and with or without BCR 54

5.9 Comparison of different Eiger Function 55

ABSTRACT

Luo, Yan M.S. ABE, Purdue University, December 2016. Mathematical Analysis of Feedback Targets of BMP signaling in Drosophila Embryonic Development. Major Professor: David Umulis, Tamara Kinzer-Ursem.

Bone morphogenetic proteins (BMPs) drive a range of cellular processes especially in the early stages of embryonic development. This family of proteins acts as one of the most important extracellular signals in development pattern formation across the animal kingdom. Cells in embryos differentiate into different cell types in response to the concentration level of BMP. This complex process is regulated by multiple regulators that serve to tune the signal response.

Extensive experimental and computational research has been performed to analyze BMP regulation in Drosophila, a widely studied model organism, and has advanced our understanding of animal development. Because of BMPs role in regulating cell growth and differentiation, identifying key players and their dynamic regulatory interactions in BMP gradient formation provides useful information to understand how BMP signaling works across the animal kingdom, and thus lead to potential treatment of related diseases and other clinical applications. Although extensive experimental study and system biology approaches like mathematical modeling have been done to investigate BMP regulations, there are still many unanswered questions on the functions of specific BMP regulators.

Specifically, in this study we aim to investigate the roles of two feedback regulators, Crossveinless-2 (Cv2) and Eiger (Egr). These two proteins cooperate with extracellular modulators like short gastrulation (Sog), and guide the formation of BMP signal gradient in Drosophila embryonic development. A genetic network containing Eiger which promotes BMP signaling and Cv2 antagonizing BMP signaling

was identified by Gavin-Smyth et.al via experimental approaches. In this report, mathematical models were built to discover the mechanism of BMP regulation with these potential feedback loops.

In order to explore Cv-2 and Eiger's roles in formation of BMP signal gradient, in this study, we developed a mathematical model with BMPs, the intracellular messenger pMad and regulators including Eiger and Cv2 for identifying potential roles of Cv2 and Eiger. A one-dimensional spatial model representing the cross-section of a *Drosophila* embryo was built. In order to compare models with multiple potential proposed mechanisms, we collected and processed data from experimental research and tested six alternative models with different proposed functions of Eiger and Cv2. Then these models were compared using Pareto frontiers, a widely-used concept in multi-objective optimization. While comparing different models, we developed a comparatively easy, yet efficient way of finding the Pareto fronts.

The results support a mechanism where i) Eiger is potentially preventing BMP releasing after binding to its receptor; ii) Cv2 is intermediating BMP by forming a complex with both BMP and its receptor, thus having a potential biphasic effect on BMP signaling, similar to Cv2 in *Drosophila* wing disc. This finding could provide new insight into the function of Eiger and Cv2, and potentially proper directions of further study.

1. INTRODUCTION

Pattern formation is a pivotal process in the development of animals. It is the process that guides cells in an embryo to organize and start to perform different functions. Patterning drives cell fate control, not only spatially but also temporally [1,2]. Among many species in the animal kingdom, many mechanisms of pattern formation are conserved. Pattern formation is often governed by a type of substance called a morphogen. Morphogens are a kind of signaling molecule, which are secreted from a local source, form a long-range spatial distribution via diffusion [3] and other transport process. Morphogens guide cells to differentiate in response to their concentrations, which in return regulate the extracellular formation of morphogen concentration gradient [4–6]. Bone Morphogenetic Proteins (BMPs) are a kind of morphogen that performs a significant role in development by transferring extracellular information to cells in embryo via binding to transmembrane receptors that trigger intracellular responses and the regulation of transcription [7]. BMPs play an important role in early stage embryonic development of *Drosophila melanogaster* [8], especially in patterning of dorsal ectoderm. It also drives development in other model organisms such as Zebrafish and *Xenopus* [9]. These regulators can interact with other players in the system and thus affect the level of BMP signal, thus forming a feedback circuit. In this report, we focus on the BMP signal gradient formation in the early stages of *Drosophila melanogaster* development, and specifically on the roles of regulator proteins.

Drosophila melanogaster is one of the most studied model organisms in biological research, especially in the field development biology.*Drosophila melanogaster* is a species of fly, in the genus of *Drosophila* and family of Drosophilidae and it's generally known as the common fruit fly. Thanks to extensive research on *Drosophila*, a great amount of information about its early stages of development is known. One

of the advantages of studying the development of *Drosophila* is that many development processes, especially morphogenesis, are widely shared across the animal kingdom. Therefore, the knowledge of *Drosophila* can be translated to more complex organisms, even vertebrates like human. Genomic research comparing human and *Drosophila* genome revealed that these two species share about 60% of genes [10]. In terms of disease-associated gene sequences, about 75% of human disease genes have matches in *Drosophila* including developmental disorder diseases and neurodegenerative disease [11]. In addition, human BMP is found to function normally in *Drosophila* [12]. Therefore, studying BMP regulation in *Drosophila* would help us explain many unanswered questions about not only evolution of BMP regulatory network, and also human BMP and BMP related diseases.

Mechanisms of morphogen-mediated patterning have been proposed since the 1950s. The study on morphogenesis, the patterning process controlled by morphogens, dates back to the 1950s and initiated by the great computer scientist Alan Turing [4]. Turing used some simple equations to show that a system whereby a homogeneous distribution of diffusible morphogens evolves into patterns like stripes or spots. Later, other mechanisms of morphogens mediated pattern formation have been proposed including the concept of Positional Information, introduced by Lewis Wolpert in 1968 [13]. The French flag model, a simple illustration of the idea of Positional information, shows how cells "know" their positional information and then perform different responses depending on the morphogen concentration gradient. It can explain mechanisms of morphogens like Bicoid [14], which are secreted from a local source and then form a concentration gradient via diffusion and interactions with other proteins. BMPs are also considered to function in such a fashion.

One of the keys to understand BMP signaling in *Drosophila* is to find out the mechanism of formation of a sharp gradient. A difference between BMPs in *Drosophila* embryo and other such kind of morphogens is that BMPs are secreted in a rather wide range in an embryo, instead of a localized source. In *Drosophila*, BMPs are secreted in a region on the dorsal side of the embryo which takes up about 40%

of embryo circumference, but in later stage the BMPs are concentrated into the dorsal midline which is only about 10% of the total embryo circumference [15–17]. It is intuitive to assume that the formation of the BMP gradient in *Drosophila* is mediated by other factors which contribute to concentrating BMPs to the dorsal midline. Experimental studies have found a number of extracellular regulators like Short gastrulation (Sog) [18] and Twisted gastrulation(Tsg) [19] which help shuttle BMPs in the extracellular space. It is also suggested that such a complex system would result in robustness and scale invariance in pattern formation [20–23].

Apart from the extracellular regulators in *Drosophila*, BMP gradient formation processes require regulation of competitive ligand binding of transmembrane surface BMP-binding proteins (SBP), Crossveinless-2 (Cv2) for example, which can bind to BMPs and form inactive complexes. Meanwhile Cv2 is a downstream gene product of BMP signaling, therefore a negative feedback loop may be formed in the system. Both computational and experimental work have been done to study its biphasic regulatory function, not only in the *Drosophila* embryo [24, 25] but also in wing disc [**?**]. In addition, Eiger (Egr), a tumor necrosis factor alpha protein, production of another downstream target gene of BMP signal, was reported to play an important role with Cv2 in the formation of a robust gradient [26].

Potential interactions associated with exchange of BMPs between receptors and Cv2 are known from study in *Drosophila* [**?**, 27] and zebrafish [28]. However, the biochemical mechanism of Eiger's role in regulating BMP signal was still largely unknown.

In order to explore Cv-2 and Eiger's roles in formation of the BMP signal gradient, in this study, we developed a mathematical model with BMPs, the intracellular messenger pMad and regulators including Egr and Cv2 for identifying potential roles of Cv2 and Egr. A one-dimensional spatial model representing the cross-section of a *Drosophila* embryo was built. In order to compare models with multiple potential proposed mechanisms, we collected and processed data from experimental research. We carried out parameter screening of multiple different models based on various poten-

tial mechanisms. Then the models were compared using Pareto front, a widely-used concept in multi-objective optimization. While doing the screening of the parameters and creating the Pareto fronts in order to compare different models, we developed a comparatively easy, yet efficient way of finding the Pareto fronts.

This report consists of a total of 6 different chapters. It is structured in a way so that readers could gain enough preliminary information from the chapter 2 and proceed to subsequent chapters in any order. The problem is set up in chapter 3. We focus on modeling and methods in chapter 4 followed by results and discussion in chapters 5. In chapter 6, we talk in brief about the conclusions we get from this project and then a couple of possible future directions to further investigate the system.

2. BACKGROUND

In this chapter we briefly go over some key concepts required for general audiences to understand the basic biological concepts associated with the proposed model in *Drosophila melanogaster*. This includes: i) describing *Drosophila* development; ii) introducing BMP governed dorsal-ventral patterning in *Drosophila*; iii)A review of existing computational modeling studies on morphogenesis, focusing on BMP in *Drosophila* embryo.

2.1 Development of *Drosophila*

As a widely and well studied model organism, *Drosophila melanogaster* is providing valuable information for developmental biologists to understand signaling pathways and pattern formation in embryonic development. Because of the conservative feature of many complex systems in animal development, knowledge gained from *Drosophila melanogaster* can be further translated to understanding similar systems in other animals, even vertebrates like human. 75% of human disease related genes can be found to have matches in *Drosophila* and these include development associated diseases [11]. One of the examples of such conservation is Bone Morphogen Proteins (BMPs) which control dorsal-ventral axis patterning in *Drosophila* embryo. Human BMP is found to perform proper function in *Drosophila* [12] embryo. This is why studying early stages (Figure 2.2) development of *Drosophila* is of great significance.

The life cycle of a *Drosophila* lasts about half a month. A fertilized egg, goes through nuclear cleavage and starts to be a blastoderm and then it comes to the stage of gastrulation to become an embryo. Figure 2.1 shows the early stages of *Drosophila* development, starting a single fertilized egg, thousands of cells of different functions and different fates are formed. This is the phase we are interested in and

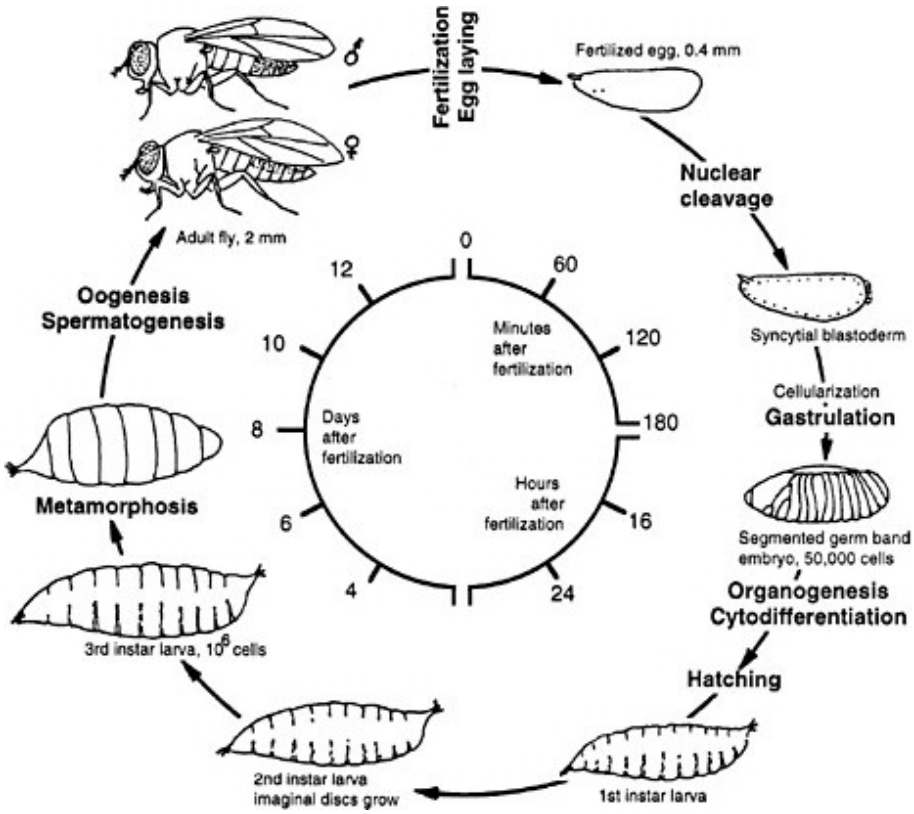

Fig. 2.1. Life cycle of *Drosophila melanogaster*: Fertilized egg goes to blastoderm and gastrulation stages after cleavage, then it becomes larva. After larva development and metamorphosis, it becomes an adult fly and restarts this cycle.(Image adapted from [29] with permission)

when we build our model. The process of BMP signal transduction is happening in Stages 5-6, which last less than one hour. After this the embryo hatches into larva. Then *Drosophila* undergoes a complete metamorphosis to become an adult. The whole life cycle is briefly demonstrated in Figure 2.1.

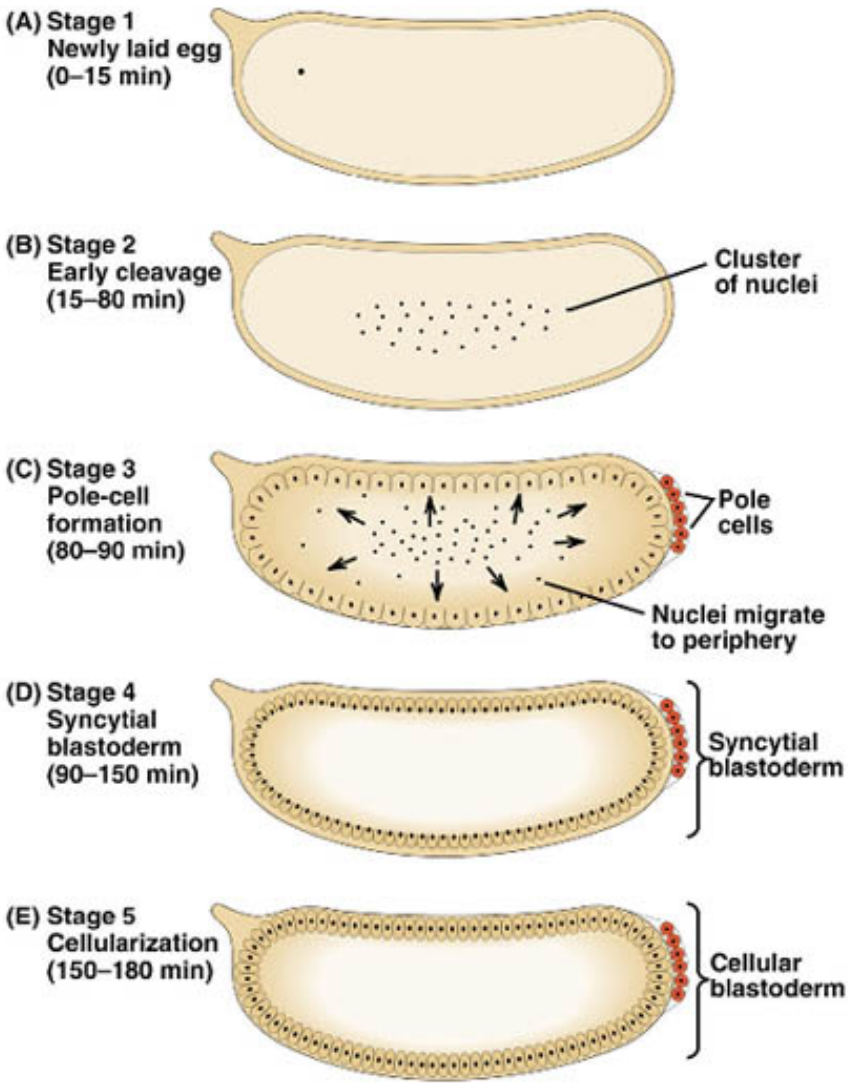

Fig. 2.2. Early stages of embryonic development: Stage 1: newly laid egg, pronuclear fusion; Stage 2: pre-blastoderm, early cell division, and start of cleavage; Stage 3: pole-cell formation; Stage 4: syncytial blastoderm and end of cleavage divisions; Stage 5: cellularization of the cellular blastoderm. (Image adapted from [30] with permission)

2.2 Morphogenesis and Morphogen

Morphogenesis, originated from the Greek word *morph* (shape) and *genesis* (creation), is the biological process which leads to cells patterning and differentiating into organized spatial distributions and thus forming organs and tissues. A morphogen is the type of molecules that controls the process of morphogenesis. BMPs form one of the most important morphogen groups in many species, and in *Drosophila* BMPs govern the dorsal-ventral patterning in the blastoderm embryo.

2.2.1 Reaction-Diffusion and Positional Information

Turing firstly used the word 'morphogen' in his milestone paper *The Chemical Basis of Morphogenesis* [4]. He referred to morphogen as the type of molecule that decides cell fates based on their concentration. In this paper, Turing proposed a simple mathematical model in which morphogens form patterns starting from a uniform distribution. A simple RD model can be described as a coupled activator-inhibitor system [31]. Both of these two component can regulate each other and themselves. A small random concentration fluctuation can cause activator to trigger a positive feedback loop at one point in space, and it would also promotes the effect of the inhibitor. One of the differences in the diffusion coefficient between the two components would cause the system to end up with a spatially-periodic shape of distribution. The formation of the periodic pattern is shown in Figure 2.3.

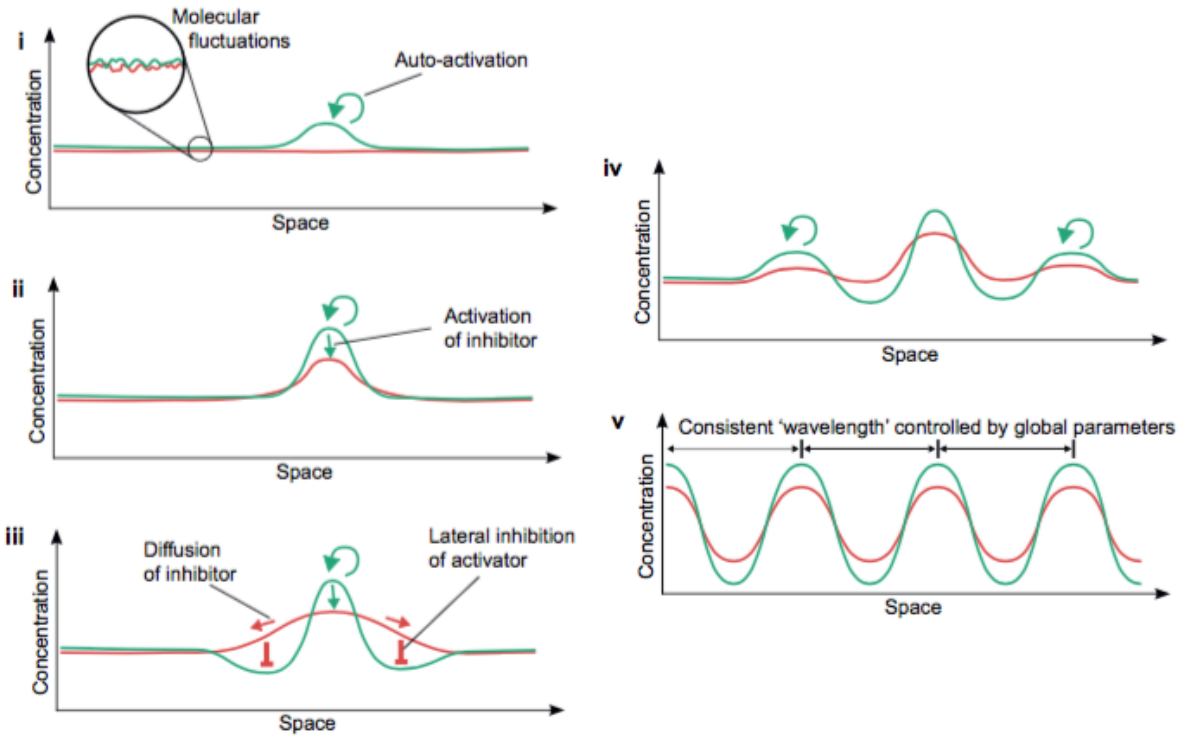

Fig. 2.3. Illustration of activator-inhibitor pair RD system. i) A random concentration fluctuation cause some cells have higher concentration of activator(green line), and a peak of activator is formed because of its auto-activation; ii) Since the activator can also promote inhibitor production, a rise of inhibitor concentration happens; iii) With faster diffusion of inhibitor, so at the peak, the inhibitor is not enough to prevent the formation of a stabilized peak from the positive feedback loop, and away from the peak, inhibitor repress production of activator; iv) Further away from the repressed region, new peaks form; v) With similar process, a spatial-periodic pattern of activator and inhibitor is formed.(Image adapted from [32] with permission)

A slightly more complicated network, BMP-Sox9-Wnt network [33] in mouse embryonic development was found to have such behavior and be responsible for limb formation. This is also a good example of a combination of experimental and computational technique in understanding pattern formation.

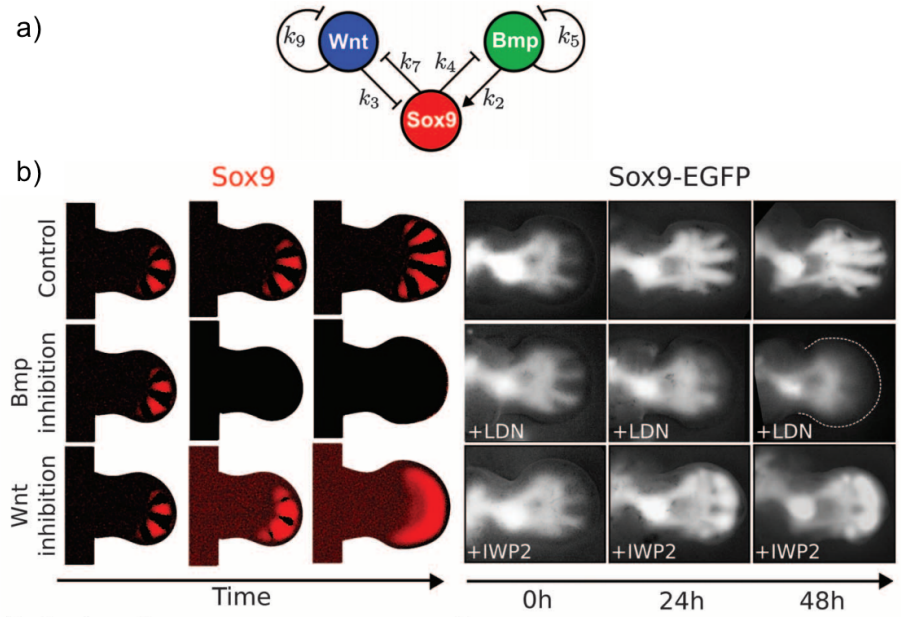

Fig. 2.4. a)Diagram of the BMP-Sox9-Wnt network. b) Left: simulation result (Sox9 distribution) based on the RD system of the network, with different perturbations. Right: Experimental results of mouse limb buds in Sox9-EGFP images with same perturbations (Image adapted from [33] with permission).

Later in the 1960s, different from Turing's interest in understanding a periodic pattern, Lewis Wolpert wanted to know how a complex pattern could form based on simple heterogeneities across the tissue. He proposed that morphogen concentration differences in space results in patterns via an additional interpretation step by cells, unlike in Turing's proposal, directly decided by the pattern of morphogen distribution. Wolpert introduced the concept of positional information (PI): the morphogen provides cell coordinates on the axis based on its concentration [13]. To be more specific, cells respond to morphogen concentration via a threshold. One important

feature of PI model is that the pattern formation process would be divided into two separate parts: the formation of PI (i.e the morphogen gradient) and the interpretation of PI (fate decision pathways in cells). The Bicoid gradient and gap genes in *Drosophila* is proof of PI based mechanism [34].

The French flag model is a concept Wolpert used to illustrate how the PI system works. Commonly morphogens are secreted from a local source and diffuse through an extracellular space in embryo during early development and thus form a concentration gradient. The positional information is passed into cells based on responses of cell to different concentration levels of morphogen. With a continuous concentration gradient and certain thresholds, cells 'know' which region of the embryo they are in and then start to differentiate into different organs or tissues.

In the French flag model, morphogens control cell fates in a threshold-dependent mechanism. Originally undetermined cells respond to different morphogen concentrations to differentiate towards different fates. For example and in brief, cells with morphogen concentration levels above Threshold 1 in Figure 2.5(b) will be controlled to express a set of 'blue' genes and thus turn into 'blue' cells.

The French flag model was then found to be applicable in *Drosophila*. The first identified morphogen, Bicoid, which is a transcription factor governing anterior-posterior axis pattern formation, was found to have a concentration gradient. Bicoid in *Drosophila*, as shown in Figure 2.6, is a good example of morphogen which can be described by French flag model. Cells along anterior-posterior differentiated into different segments, which can be demonstrated by different RNA levels of genes *orthodenticle, hunchback*, and *krüppel*.

Although these two models differs in some way, they are never exclusive to each other, in fact, combination of these two models would be beneficial to many biologists in understanding the true nature of pattern formation. In Wolpert's model, the positional information is 'coded' in morphogen gradient, but how the gradient is formed remains an open question. However, RD model does a good job in interpreting the formation of morphogen pattern itself. So in a scheme that RD system works prior

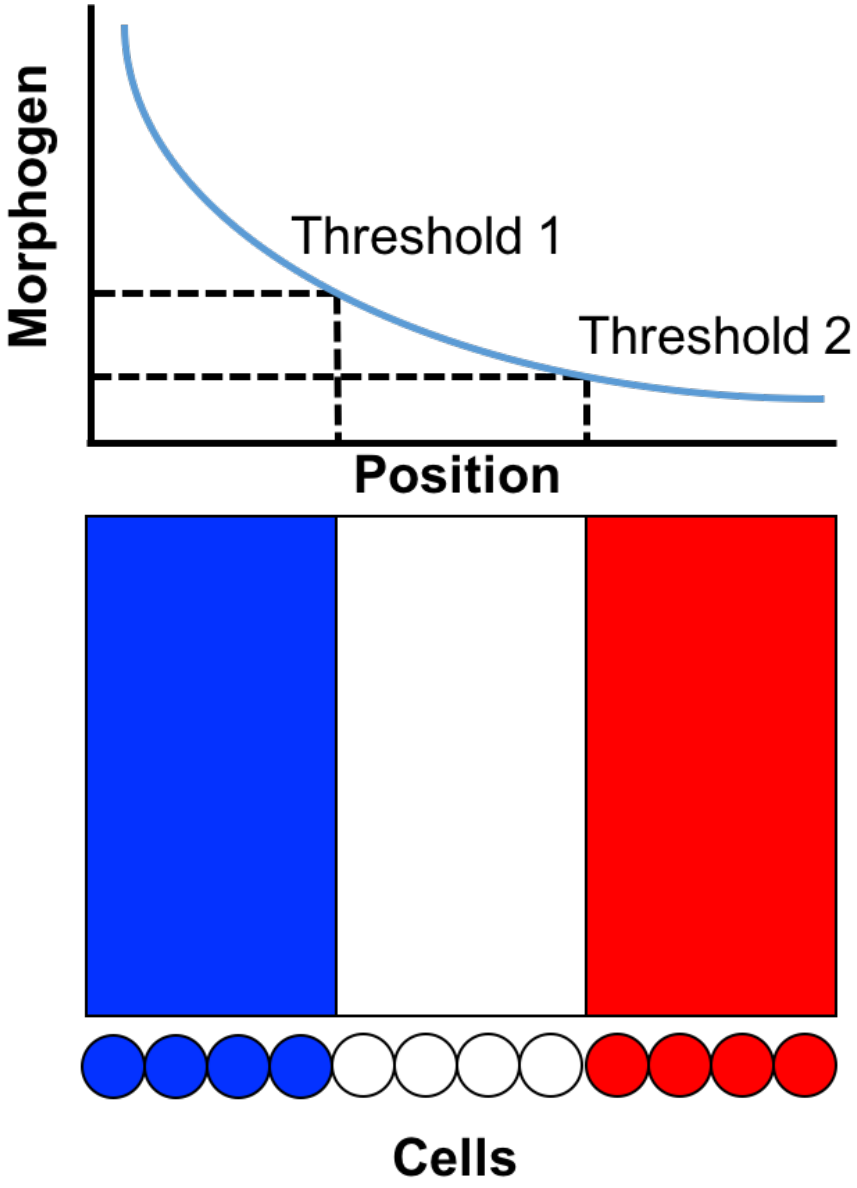

Fig. 2.5. French flag model in which two different threshold concentrations of a morphogen elicit three distinct responses.

to, or in parallel with PI system, it is quite promising to build better model. As a result, based on these two basic, abstract models, more specified models have been proposed to explain mechanisms by which morphogens work in specific organisms. In these models, the abstracted general scheme in RD and PI system is specified

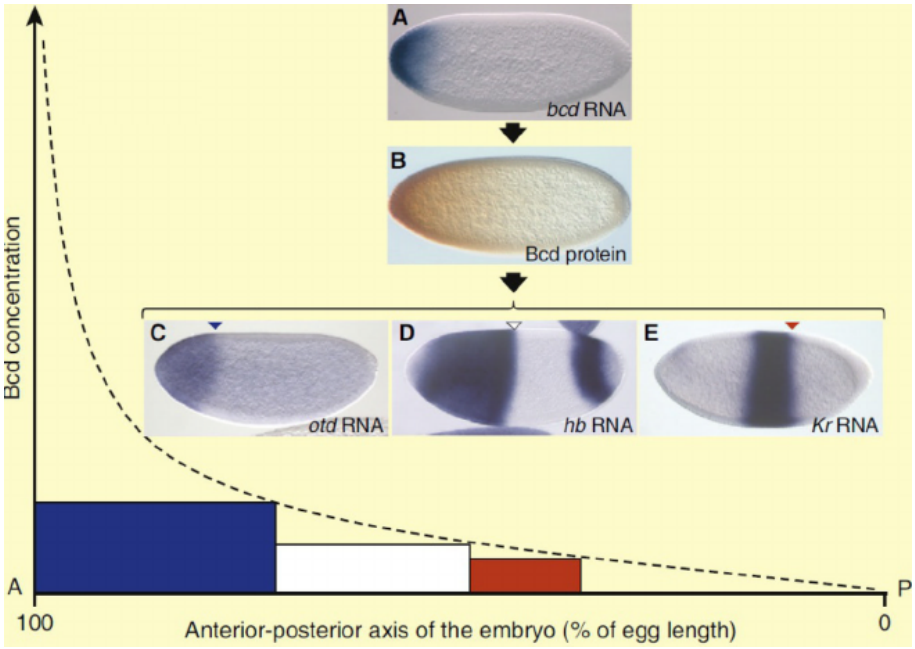

Fig. 2.6. The French Flag model explaining Bicoid mediated Anterior-Posterior patterning in *Drosophila* embryo.(Adapted from [34] with permission)

by identifying morphogens and their regulators, studying kinetics and topologies of networks, and discovering intracellular signal transduction pathways. BMP signaling system, described in detail in the next section, is an example of combination of these two ideas.

2.2.2 BMP in *Drosophila* Embryonic Development

In *Drosophila*, dorsal-ventral axis patterning is administered by Bone Morphogen Proteins (BMPs) [35, 36]. BMP governed D-V patterning is also found in a wide range of animals like Xenopus [9]. BMPs can bind to cell-surface receptors and then activate intracellular signal pathways leading to regulation of transcription of target genes. Different levels of this signal would therefore lead to different levels of transcription of genes through two mechanisms: direct activation of target genes and

relief of repression from a sequence-specific transcriptional repressor Brinker (Brk) [37]. In this way, BMPs govern cells to differentiate and control growth of cells in dorsal and ventral regions of the embryo. In addition, this formation process is regulated by extracellular proteins, surface BMP-binding proteins and potentially some intracellular proteins.

BMPs are transforming growth factor beta (TGF-β) family proteins which play a key role in development. BMP was found to be able to induce bone formation and then found to have important function in early stages of development [38]. In *Drosophila*, there are two BMP ligands: Decapentaplegic (Dpp, a human BMP2/4 ortholog) and Screw (Scw, a human BMP5/7 homolog). BMPs are functioning in forms of heterodimers constructed by Dpp and Scw. In order to transduce signals into cells, a BMP hetererdimer binds with a transmembrane heterotetrameric receptor which is formed by two Type I receptors, Saxphone (Sax) and Thickveins (Tkv), and two Type II receptors (Punt) [9,39]. With BMP bound, Type II receptors phosphorylate transcription factor Mothers against dpp (Mad) in the cytoplasm. Phosphorylated Mad (pMad) forms a complex with cofactor Medea then enters the nucleus of the cell [40]. This pMad-Medea complex can regulate transcription of target genes. This general diagram is shown in Figure 2.7 (a).

An important difference between the two morphogens, Bicoid and BMP, is that Bicoid is a transcription factor itself but BMP controls patterning by an intracellular messenger pMad. Therefore concentration of pMad is the representation of BMP signal, rather than concentration of BMP ligands.

BMPs in *Drosophila* are secreted in a rather large range at the dorsal side of the embryo which takes up about 40% of total cross-section circumference of the embryo. In order to concentrate BMP in dorsal-most region of the embryo, there is a shuttling system. Short gastrulation (Sog) is secreted in ventral regions and it can form an inhibitory complex with Twisted gastrulation (Tsg), and this complex then binds BMP heterodimer, ending with an inactive complex [**?**,41]. Protease Tolloid (Tld) is secreted in the dorsal range, so when the inactive shuttling complex diffuses to the

dorsal region, Tld cleaves Sog and thus releases the BMP heterodimer [42, 43], which can bind with receptors and activate intracellular signal pathway.

With this shuttling system, BMPs concentrate mostly to cells close to the dorsal midline. Such a concentrated gradient makes cells in dorsal midline have less chance of misinterpreting BMP signal with BMP concentration over threshold. However, other than shuttling of BMP heterodimers, the formation of the final BMP signal gradient, or pMad concentration gradient, requires other regulators like surface BMP-binding proteins and potentially some intracellular proteins. The two regulators, Cv2 and Eiger, are regulating the pMad distribution in the signal transduction step. This report adopted mathematical modeling to investigate these two proteins, since mathematical modeling was an important and useful tool in understanding BMP signal pathway in *Drosophila*, as reviewed in the next section.

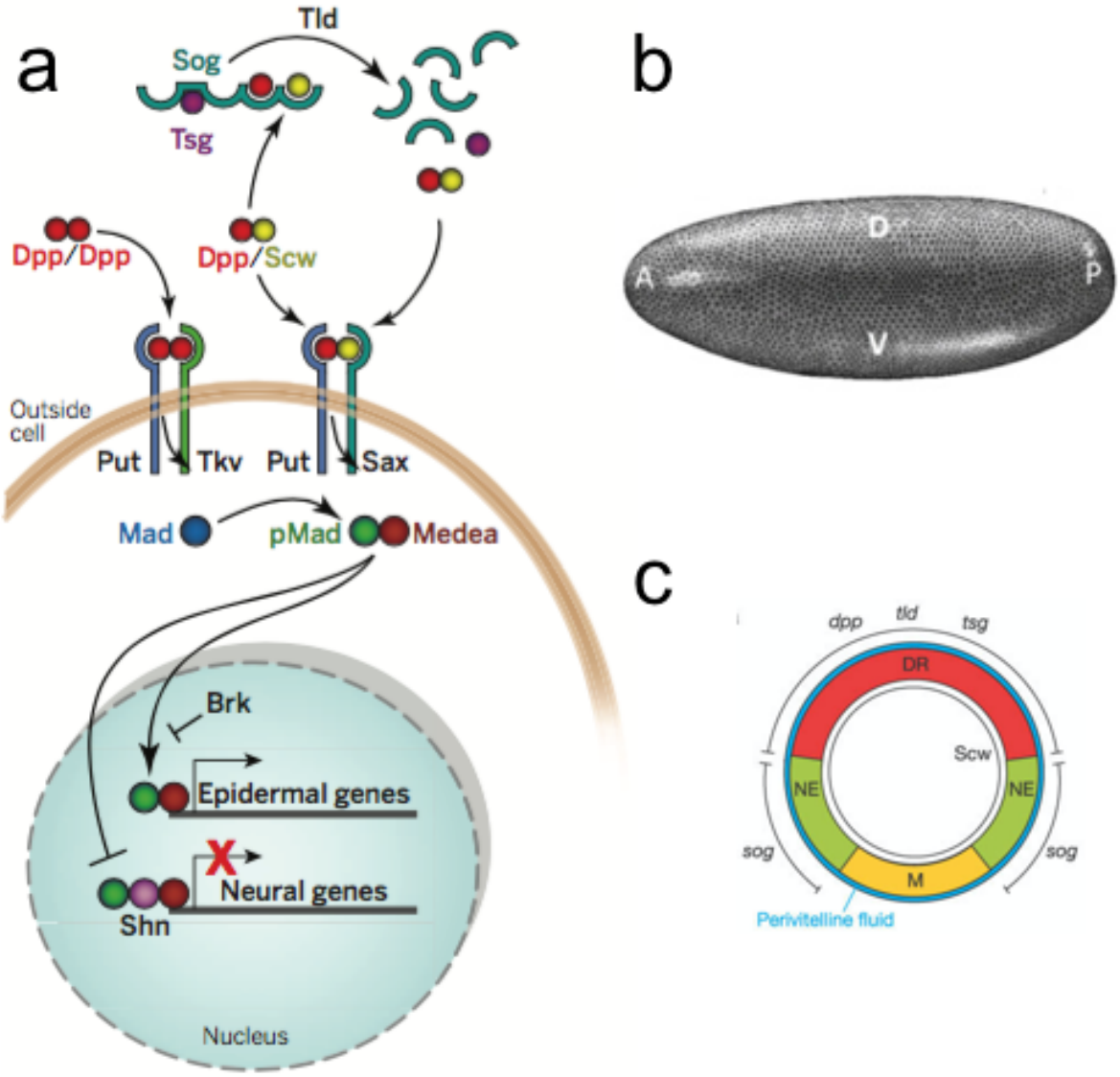

Fig. 2.7. a) Diagram of BMP signaling pathway in *Drosophila*, description in text (Image adapted from [44] with permission). b) Axes and geometry of a Drosophila blastoderm embryo(A: anterior, P: posterior, D: dorsal, V: ventral) (Image adapted from [45] with permission). c) Cross-section of a Drosophila embryo in the early stages of development showing the different regions of gene expression (Image adapted from [8] with permission).

2.3 Mathematical Models of BMP in *Drosophila* Embryo

Models were proposed on the extracellular shuttling system which consists of inhibitors Sog and Tsg and protease Tld. Models [45,46] showed that shuttling of BMP by inhibitors is essential for the system to establish a transient and intense BMP-Receptor gradient. In addition, these models focused on reproducing the robustness to partial loss of molecules in the system. In these models, the BMP transport mechanism in extracellular space was studied and some predictions were made on diffusivity of BMP and function of Sog, Tsg and Tld in shuttling BMP to dorsal region, although some predictions don't agree with experimental findings [16]. A study specifically on transport of morphogen based on abstract models [47] compared different mechanisms including free diffusion, hindered diffusion, etc. The investigation on facilitated shuttling predicted competition between the shuttle and other regulators located on cell membrane.

Feedback with surface BMP-binding proteins triggered by the intracellular BMP signal were found to be responsible for the formation of BMP signal gradient [24]. In addition, it was found that feedback loops are essential in the formation of sharp spatial distribution of BMP:Receptor complexes. With feedback loops included, BMP signaling contracts to dorsal midline of the embryo because of a spatial bistability in the system. [24]. This feedback loop was found experimentally to be conducted by intracellular gene regulation [16], showing that feedbacks lead to refinement of both pMad, the intracellular messenger of BMP signal and BMP itself.

Step by step, unknown parts in the whole network were unveiled and used in later models. Separate modules including i) BMP ligands form dimers; ii) BMPs are transported by extracellular shuttling system with the assistance of Sog, Tsg, and Tld; iii) the signal is transferred into cells from BMP:Recptor complex to pMad which then regulates downstream gene product, thus providing the feedback loop. These three separate modules were then combined to build a spatial-temporal model

illustrating the process to identify that surface BMP-binding proteins form feedback loop which provides robustness to the system. [22, 24].

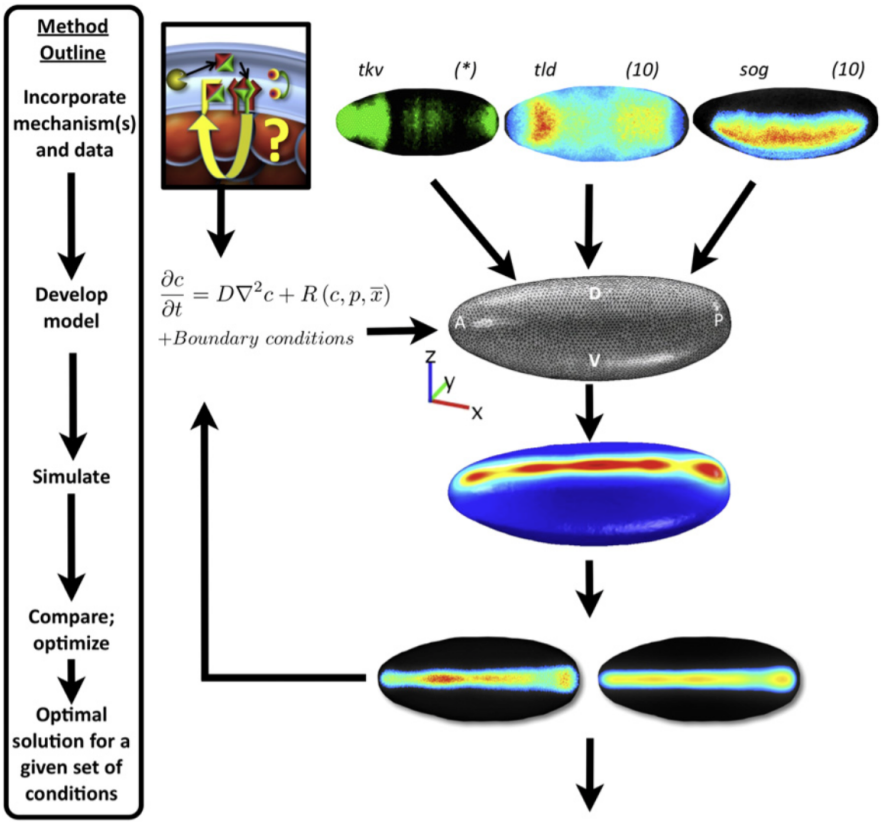

Fig. 2.8. Workflow for the Development of a 3D whole embryo-scale model. Geometric information are coded into a 3D representation of the Drosophila embryo. Each model representing different proposed mechanisms are then simulated yielding the distribution of all proteins in the system. Models are trained from data extracted from pMad staining images of WT and 8 mutants. Differences between model output and image data are used to compare models quantitatively. (Image adapted from [8] with permission)

Based on the findings about the three modules of the system, a whole embryo scale 3D model [8] was incorporated to test several different potential feedback mechanisms, including feedback on Tld processing rate or BMP receptor associating rate. Model output was compared with experiment results, showing that a secreted surface BMP-

binding protein, such as Cv2, affects the binding process of BMPs and receptor with data. 1D and 3D model based on this proposal also find that such a bistable switch like system makes sure that with limited amount of ligand, cells near the dorsal midline can competitively contract ligand to maintain high signal state while the other cells resting in low signal state. With the help of the feedback loop, a canalized signal, or a sharpe narrow gradient is formed. At the same time, such a system provides essential robustness when the extracellular system shuttles the ligands to a rough region where a certain level of error in BMP gradient is tolerated.

BMP signaling has also been modeled in other organs or via different approaches. Such a system is also been studied in *Drosophila* wing discs [**?**] both experimentally and computationally. Another investigation on robustness from positive feedback was done via a stochastic modeling approach study [23], and it showed that noise reduction feature of Cv2 binding of BMP. Cross-talk between BMP signaling and other pathways was also studied by combination of mathematical modeling and experiments. A model focusing on intracellular gene regulations of Gurken pathway and BMP signaling system linked by transcription factor Brinker predicted the presence of an additional positive feedback loop between BMP signaling and BMP receptor expression [48]. Another modeling study [49] comparing BMP signal in different species of *Drosophila* proposed that level of BMP receptor expression determined final BMP gradient.

Models reviewed above focused on different parts of the BMP signaling system and different mechanisms, in form of explicit protein interactions or abstract feedback, were proposed to i) increase robustness of the system. ii)reproduce wild-type and mutant data. Experiments in parallel with or after computational models either confirm model predictions or lead to new directions of modeling. In 2013, experimental results [26] validated the modeling results and confirmed the robustness provided by the Cv2 feedback loop. It was found that Cv2 along with Eiger, another downstream target gene product of pMad, promotes signal canalization, with both genes knocked out, pMad distribution have much greater variability. This also leads to the work in this report, which is to identify the roles of Eiger in the system. The inte-

gration of experiments and mathematical modeling, ensures that the understanding of BMP signaling in *Drosophila* embryos moves forward.

In these models, there are two common ideas: i)robustness is a desirable feature of a signal transduction system, because a robust system increase the chance of an embryo surviving from partial loss of one or more functioning proteins. ii)BMP:Receptor complex was considered as the quantified readout of BMP signal, although in experiments the technique measures the downstream pMad. Therefore intracellular regulators which work on pMad level might not be discovered, one of the protein we focused on in this report, Eiger, might be one of these regulators. In addition, Eiger mutant showed high variability in pMad distribution, therefore robustness of pMad, the direct signal readout, need to be studied.

3. PROBLEM DESCRIPTION

As described above, the BMP governed D-V patterning process is based on BMPs transferring extracellular information to cells in the embryo by specifically binding with receptor complex. This patterning process depends on the formation of the sharp gradient of BMP in *Drosophila*, and pure diffusion of BMP is unlikely to form such a sharp gradient because of the broad range of BMP secretion. However, experimental research has found that there are actually other regulators that are responsible for the gradient formation. Genetic experiments showed that by knocking down these regulators, the formation of BMP gradient is perturbed, some of them showed weak signal or signal with much noise. In fact, the extracellular BMP signal regulatory network is rather complex, with a number of regulators and BMP binding proteins [22]. Computational modeling is an ideal method to investigate the system with many potential feedback loops because of its efficiency and ability to test alternative hypotheses. Even whole embryo scale analysis of different feedback loops on BMP signal pathway can be performed to identify consistent feedback loops existing in nature [26]. Using computational modeling we are able to address many unanswered questions regarding regulators.

For a single cell we can consider BMP as an input to the pattern formation system and its intracellular messenger, pMad, which is directly performing target gene promotion or inhibition, can is the measured readout. In such way, the final readout, is approximated by pMad concentration. Crossveinless-2 (Cv2) and Eiger (Egr) are two molecules which both are downstream target gene of pMad and in return regulate BMP signal gradient.

3.1 Regulation of Crossveinless 2

Cv-2 is known to regulate BMP signal transduction in developing *Drosophila* wing discs, Zebrafish embryos, and *Xenopus* embryos. The biochemical research found that Cv2 competitively binds with BMP heterodimer such that the heterodimer cannot interact with Type I receptors. In addition, interaction between BMP, Type I receptor, and Cv-2 leads to another intermediate complex which is composed of these three molecules. Both the BMP:Cv2 and BMP:Receptor:Cv2 complexes are inactive and unable to signal, so in this way the number of active BMP:Receptor complexes on the cell membrane is affected by the presence of Cv2 molecules. The interactions are shown in Figure 3.1

With such a competitive binding molecule, the dynamics of this system can be very complicated, the actual effect of Cv2 can promote or inhibit BMP signaling, depending on kinetic parameters or the amount of Cv2 in the system. A study combining experimental and computational research showed that Cv2 is a biphasic regulator that functions on concentration-dependent fashion [**?**]. Such a biphasic regulating feature makes Cv2 a potential source of bistability and in such a way provides robustness to the system [25].

However, it is unclear what the kinetic rates for these three molecules are and whether the receptor can bind BMP ligand when the ligand is captured by Cv-2 [**?**, 50, 51]. Computational studies suggested that Cv-2 can be functioning as exchanging BMP via the intermediate trimer and in this way regulates the stability of the system, even though structure biology research suggested otherwise [51]. With more data showing the actual pMad distribution of Cv-2 mutant embryos [26] it might help to answer this question using computational methods.

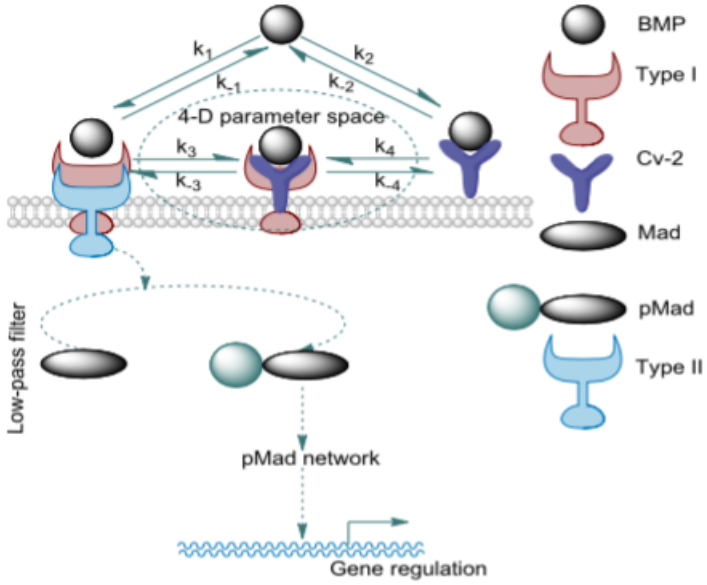

Fig. 3.1. Diagram of interactions between Cv2, BMP and BMP receptors. BMP can bind both Type I receptor and Cv2 and there is an intermediating complex formed with BMP, Cv2 and Type I receptor.(Image adapted from [25] with permission)

3.2 Eiger Promoting BMP Signal

Eiger is a homolog of tumor necrosis factor-alpha protein which is an essential part of the JNK (Jun N-terminal kinase) pathway in *Drosophila*. Study on Eiger is limited compared to Cv2, especially in details of potential mechanisms. Eiger leads to ectopic apoptosis through JNK pathway activation and thus plays an important role in damage-induced neuronal apoptosis [52]. Also, as a fat-body derived signal released in the hemolymph in response to starvation, Eiger is an adipokine that reduces the expression of insulin-like peptides by remotely acting on its receptor Grindelwald locally expressed in the brain insulin-producing cells [53].

Eiger's effect on *Drosophila* BMP signal was found through a series of genetic experiments which demonstrated that Eiger, is a downstream target gene of BMP signal, and acts in the positive feedback loop to promote signaling, while Cv2 si-

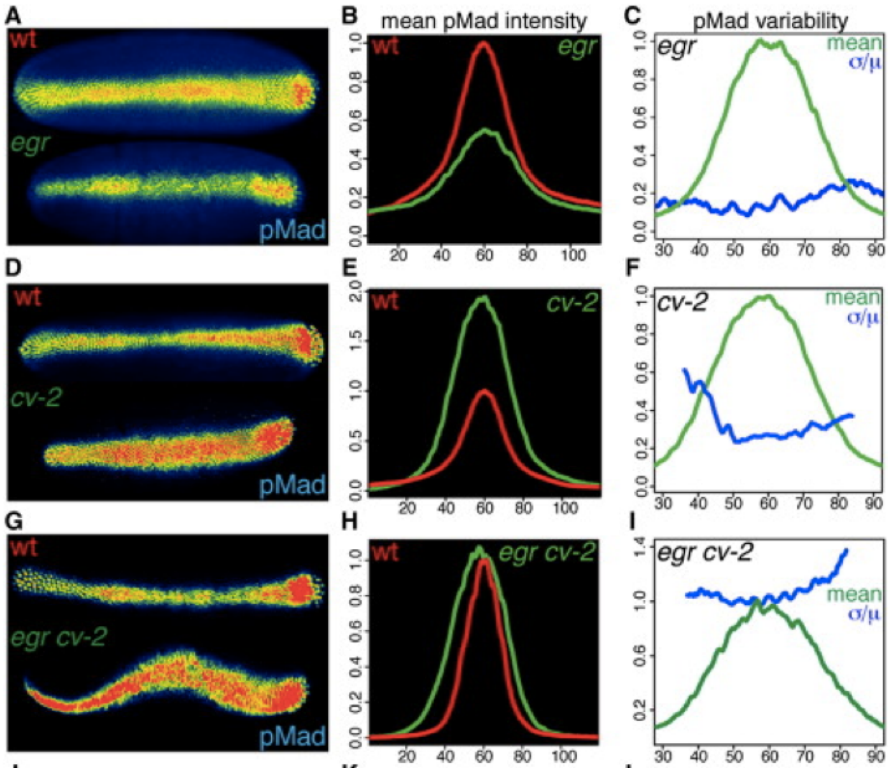

Fig. 3.2. pMad Staining of Eiger and Cv2 mutant embryos: (A I) dorsal view pMad staining images (A, D and G), mean intensities (B, E, and H), and variability (C, F, and I) of*egr* embryos (AC), 8 *cv-2* embryos (DF), 15 *egr cv-2* embryos (GI), the corresponding control group (wild type).(Image adapted from [26] with permission)

multaneously antagonizes signaling. Moreover, the detailed mechanism by which the promotion acts remains unclear. In this report we use mathematic modeling to address these unanswered questions.

A previous study [16] on visualizing receptor-bound BMP showed that the extracellular shuttling system alone is not enough to construct a sharp gradient of BMP signal, and there exists a positive feedback by intracellular gene regulation to produce a spatially bistable signal. More importantly, the experiments showed mutant of *zerknüllt*, the target of pMad and upstream gene of *eiger* and *cv2*, causes BMP signaling to broaden and decrease inxw intensity.

4. METHODS

In order to investigate the functions of Egr and Cv-2 using computational models, first the experimental results are studied to identify general effect of these two regulators and with this limited information, a simplified local model for a single cell was built to study the general dynamics and bistability of the system.

Next, we included spatial information and diffusion of molecules are included in the model to study the impact of the local models on pattern formation. This model also took complex interactions between Cv2 and BMP or receptors. Based on the 1-Dimensional spatial model, different potential functions of Egr are proposed to construct alternative networks in order to find which one have the best fit with experimental data.

Experimental data, mainly in the form of pMad staining images from published literature was collected to validate the models. Images of dorsal view immunofluorescent images were processed to extract quantified data and calibrated using more trustworthy data.

In order to compare different models with multiple data we used Pareto Optimization, a widely used multi-objective optimization.

4.1 Local Model

The basic information we get from the experimental data is: i) Cv2 inhibits BMP signal; ii) Eiger promotes BMP signal; iii) Both Cv2 and BMP are downstream target gene of BMP signal, to be more specific, both genes are promoted by pMad. Starting from these findings we built a local model. Considering BMP as the input of the system and pMad as the readout, a local ODE model was built and implemented using Matlab. The diagram of this simplified model is shown below in Figure 4.1.

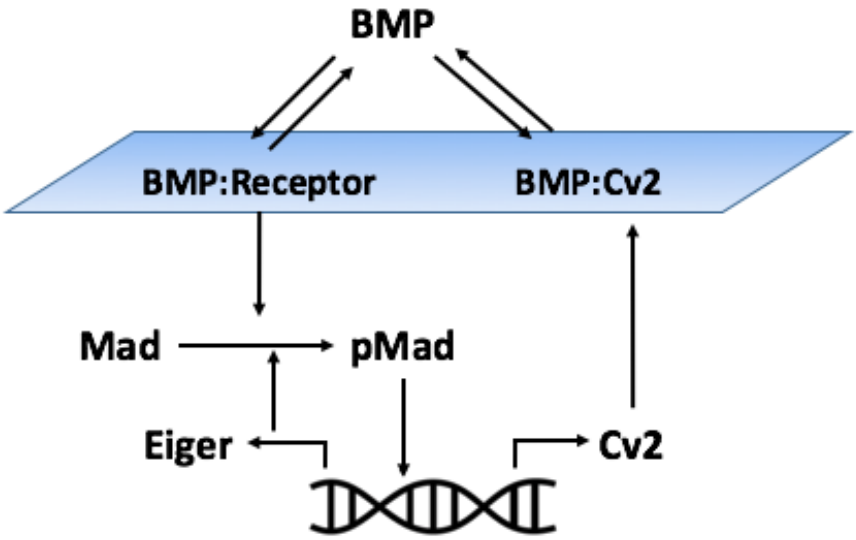

Fig. 4.1. Diagram of Local Model

In order to make the model simpler, some assumptions are made. And the notations of each variable and their related information and notations are listed:

BMP [**B**] Bone Morphogen Protein. Although in *Drosophila*, BMPs works as heterodimers of Dpp and Scw, but we assume the formation of these two ligands are fast so that a single variable is used in modeling.

Receptor [**R**] Similarly, kinetics with BMP:Type I receptor with Type II receptor is fast, so that in here we use one variable to illustrate the receptors.

BMP:Receptor [**BR**] BMP:Receptor complex.

BMP:Cv2 [**Cv2**] BMP:Cv2 complex.

Eiger : [**E**] Eiger.

Cv2 : [**C**] Crossveinless-2.

pMad : [**P**] Phosphorylated Mad.

Reactions and interactions in the model are as follows:

$$\Phi \xrightarrow{\phi_B} B, B \xrightarrow{\delta_B} \Phi$$

$$\Phi \xrightarrow{\phi_E} E, E \xrightarrow{\delta_E} \Phi$$

$$\Phi \xrightarrow{\phi_C} C, C \xrightarrow{\delta_C} \Phi$$

$$B + R \xrightarrow{k_1} BR, BR \xrightarrow{k_{-1}} B + R$$

$$B + C \xrightarrow{k_2} BC, BC \xrightarrow{k_{-2}} B + C$$

$$Mad \xrightarrow{phosphorylation} pMad$$

$$pMad \xrightarrow{dephosphorylation,degradation} \Phi$$

In the reactions above, the production rate of Eiger and Cv2 are positively regulated by pMad, to illustrate this promotion effect, second degree hill equation is used (Shown in ODEs). k_1, k_{-1}, k_2, k_{-2}, are binding and dissociation coefficients. ϕ_B, is the production rate of BMP. ϕ_C and ϕ_E are the basal production level of Cv2 and Eiger.K_E and K_C are the half occupation term in hill equation. δ_B, δ_C, δ_E, δ_{BR} and δ_{BC} are degradation rate of molecules. k_s and k_{se} are the phosphorylation factor of phosphorylation intermediated by BMP:Receptor or Eiger. k_d is the dephosphorylation rate of pMad. $[R]_{total}$ is the total amount of Receptor.

$$\frac{dB}{dt} = \phi_B - k_1 \cdot B \cdot R + k_{-1} \cdot BR - k_2 \cdot B \cdot C + k_{-2} \cdot BC - \delta_B \cdot B$$
$$\frac{dC}{dt} = \frac{\phi_C P^2}{P^2 + K_C^2} - k_2 \cdot B \cdot C + k_{-2} \cdot BC - \delta_C \cdot C$$
$$\frac{dE}{dt} = \frac{\phi_E P^2}{P^2 + K_E^2} - \delta_E \cdot E$$
$$\frac{dBR}{dt} = k_1 \cdot B \cdot R - k_{-1} \cdot BR - \delta_{BR} \cdot BR$$
$$\frac{dBC}{dt} = k_2 \cdot B \cdot C + k_{-2} \cdot BC - \delta_{BC} \cdot BC$$
$$\frac{dP}{dt} = k_s \cdot Mad \cdot BR + k_{se} \cdot Mad \cdot E - k_d \cdot P$$
$$[R]_{total} = R + BR$$

The parameter values are referred to previous modeling work in our lab and simulations are performed using Matlab built-in ODE solver ODE-15s [54, 55].

4.2 Bistability Analysis

In order to study the bistability of the system since both Cv2 and Eiger are forming feedback loops which end up with non-linear terms in the system, MatCont [56], a continuation analysis tool was adopted. Before using MatCont to study the stability of the system, analysis based on steady-state equations are conducted to prove that if considering BMP as an input to one cell and pMad as readout, there might be bistability provided by Eiger. Software set up is shown in Figure 4.2.

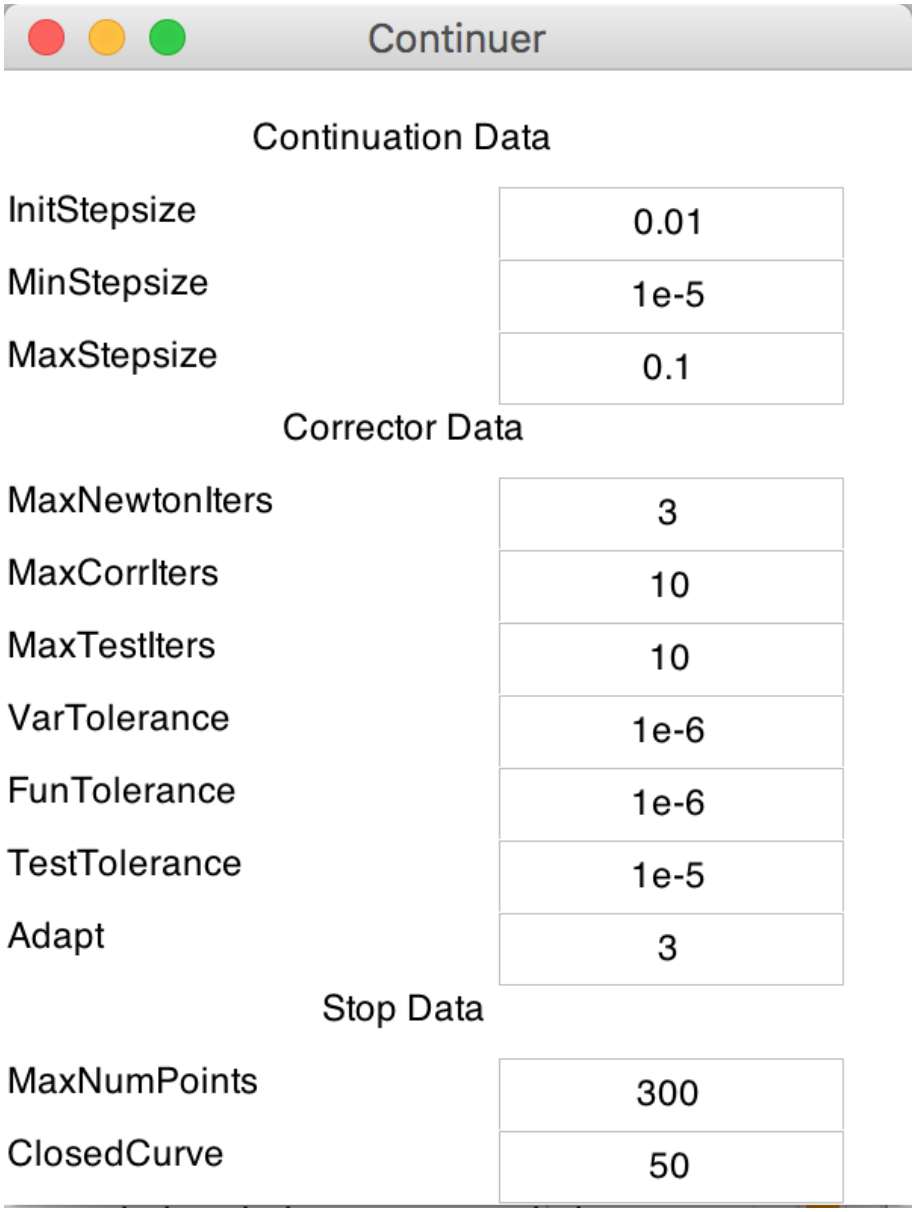

Fig. 4.2. Set up parameter values for continuation analysis in MatCont

4.3 One-Dimensional Spatial Model

To build a model with diffusion and extracellular shuttling systems considered, a 1D spatial model was built based on reaction diffusion scheme. Reaction-diffusion system is widely used in modeling biological mass transport system. The diagram of our current model is shown in Figure 4.3

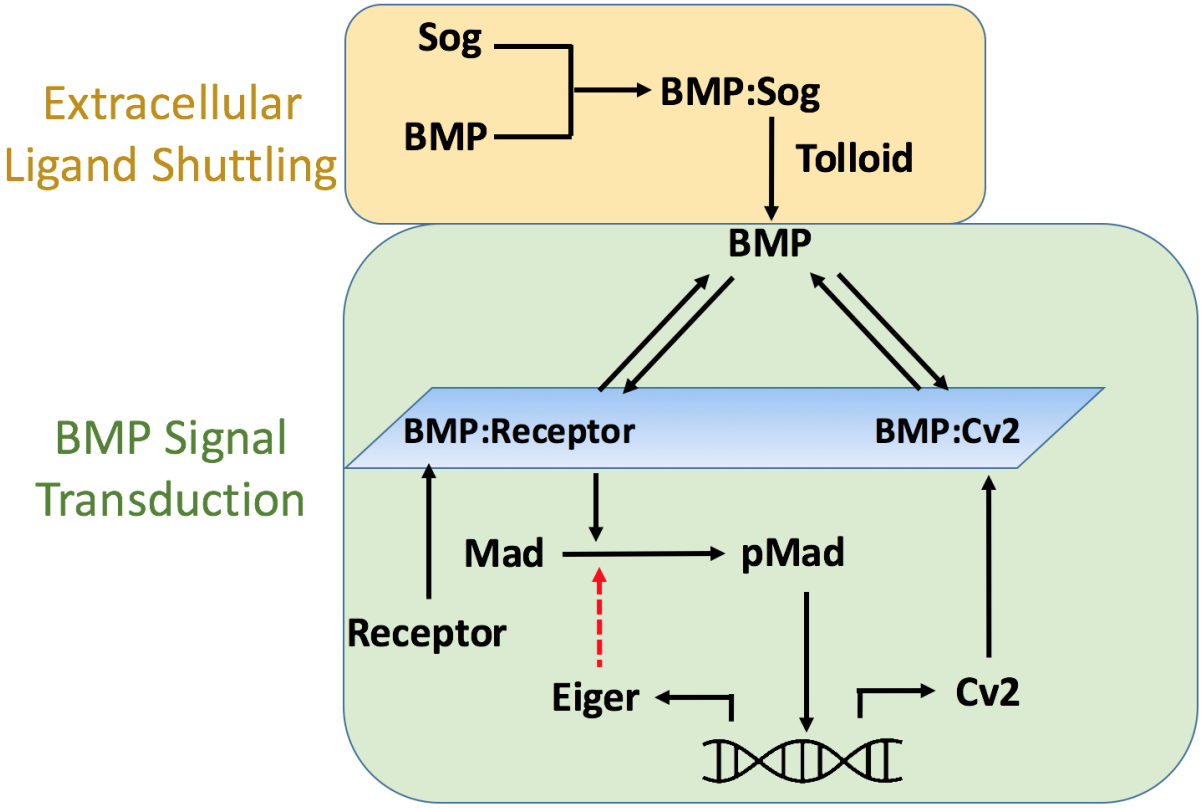

Fig. 4.3. Diagram of Spatial Model

Some additional variables:

Sog [**S**] Short gastrulation, inhibitory molecule. Although Sog is inhibiting BMP by forming a dimer with another molecule Tsg, we consider the binding of these two molecules as fast so that a single variable is enough to demonstrate the process.

Sog:BMP [**SB**] Complex of inhibitor binding with BMP, this complex is inactive and can transferred via diffusion. This complex can be cleaved by Tolloid, and release BMP

PDEs based on the system

$$\frac{\partial B}{\partial t} = D_B\frac{\partial^2 B}{\partial x^2} + \phi_B - k_1 \cdot B \cdot R + k_{-1} \cdot BR - k_2 \cdot B \cdot C + k_{-2} \cdot BC - k_3 \cdot B \cdot S + k_{-3} \cdot SB + \lambda Tld$$
$$\frac{\partial S}{\partial t} = D_S\frac{\partial^2 S}{\partial x^2} + \phi_S - k_3 \cdot B \cdot S - k_{-3} \cdot SB - \delta_S \cdot S$$
$$\frac{\partial C}{\partial t} = \frac{\phi_C P^2}{P^2 + K_C^2} - k_2 \cdot B \cdot C + k_{-2} \cdot BC - \delta_C \cdot C$$
$$\frac{\partial E}{\partial t} = \frac{\phi_E P^2}{P^2 + K_E^2} - \delta_E \cdot E$$
$$\frac{\partial BR}{\partial t} = k_1 \cdot B \cdot R - k_{-1} \cdot BR - \delta_{BR} \cdot BR$$
$$\frac{\partial BC}{\partial t} = k_2 \cdot B \cdot C + k_{-2} \cdot BC - \delta_{BC} \cdot BC$$
$$\frac{\partial SB}{\partial t} = D_{SB}\frac{\partial^2 SB}{\partial x^2} + k_3 \cdot S \cdot B - k_{-3} \cdot SB - \lambda Tld \cdot SB$$
$$\frac{\partial P}{\partial t} = k_s \cdot Mad \cdot BR + k_{se} \cdot Mad \cdot E - k_d \cdot P$$
$$[R]_{total}(x) = R(x) + BR(x)$$

$BoundaryCondition$:

$$\frac{\partial B}{\partial x}|_{x=0} = \frac{\partial B}{\partial x}|_{x=L} = 0$$
$$\phi_B(x)|_{x=0-125\mu} = \phi_B$$

In the equations above, D_B, D_S and D_{SB} are diffusion coefficient of corresponding molecules. $D_B\frac{\partial^2 B}{\partial x^2}$ shows the diffusion term at any point in the system. $k3$ and k_{-3} are

binding and dissociation coefficient between BMP and Sog. λTld is Tolloid process rate.

4.3.1 Finite Difference Scheme

The PDE model is discretized using finite difference scheme. In the dimensionless form of equation for Sog, the spatial domain is subdivided into a total of N uniformly distributed mesh points:$h = \frac{1}{N}$ where $x_i = i \cdot h$ and $i = 1, 2, ...N$. Lets characterize the time-dependent value of S as $S_i(t) = S(x_i, t)$, then the discretized version of the equation for B can be written as:

First node:

$$S_1(t) = \frac{S_0(t) - 2S_1(t) + S_2(t)}{h^2} + \phi_S(1) - k_3 \cdot B_1 \cdot S_1 - k_{-3} \cdot SB_1 - \delta_S \cdot S_1$$

Middle nodes:

$$S_i(t) = \frac{S_{i-1}(t) - 2S_i(t) + S_{i+1}(t)}{h^2} + \phi_S(i) - k_3 \cdot B_i \cdot S_i - k_{-3} \cdot SB_i - \delta_S \cdot S_i$$

Last node:

$$S_N(t) = \frac{S_{N-1}(t) - 2S_N(t) + S_{N+1}(t)}{h^2} + \phi_S(N) - k_3 \cdot B_N \cdot S_N - k_{-3} \cdot SB_N - \delta_S \cdot S_N$$

Two fictional nodes, Node 0 and Node $N + 1$ are approximated by the concentration of proteins in the first node and the last node. PDEs of other variables are discretized similarly. Cell length will be treated equal to the mesh stem h, so each cell in the system would have one ODE system in the format as above. The diffusion terms for cells located at beginning and end of the region would be modified for approximation. The number of mesh points chosen is 55, and these 55 points represent half of an embryo, starting from dorsal midline. Half of embryo cross-section peripheral is approximated as 275 microns so mesh step is $h = 5$ microns. Production term of BMP, Sog and the parameter λTld are functions of x in order to show the distinct domains of gene expression as shown in Figure 2.5 (c). In this model, BMP has uniform production rate in the range 0-125 microns, Sog has uniform production rate in the range 125-225

microns, and Tld has pre-pattern in the same range with BMP production. Since the cross-section of *Drosophila* embryo is symmetric, so it is only needed to model half of the peripheral.

4.3.2 Proposed Mechanisms

The 1D-Spatial Model described above is just the first proposed functions of Eiger. As mentioned in the Problem Description chapter, the true biochemical feature of Eiger is still unknown and there is debate on Cv2's intermediating role in the kinetics. So in order to find the most consistent models, some alternatives are made for further testing and validating. Below in Figure 4.4 are the diagrams of 6 major alternatives tested.

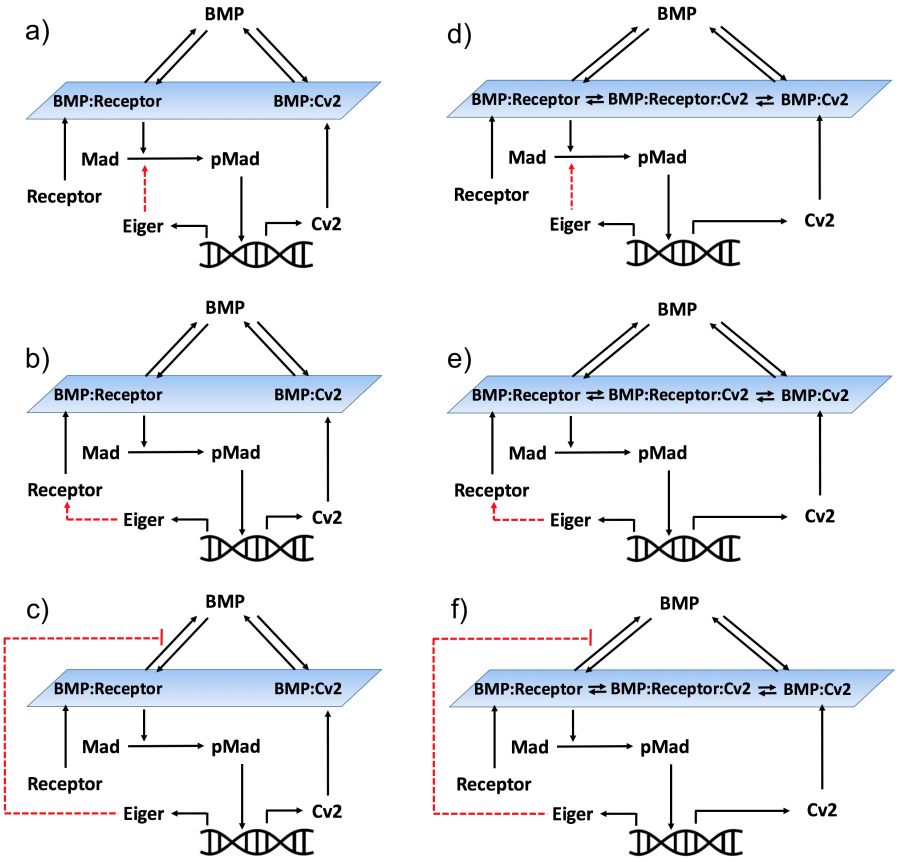

Fig. 4.4. Diagrams of Major Alternative Networks: a) Eiger promoting phosphorylation/No BCR; b) Eiger promotes production of receptor/No BCR; c) Eiger inhibits dissociation of BR/No BCR; d) Eiger promoting phosphorylation/With BCR; e) Eiger promotes production of receptor/With BCR; f) Eiger inhibits dissociation of BR/With BCR

Three major possible Eiger function models were made:

Ks+ Eiger promoting phosphorylation of Mad.

Receptor+ Eiger promoting amount of Receptor.

Koff- Eiger inhibiting dissociation of BMP:Receptor Complex.

Ks+ is the most intuitive guess of how Eiger promotes level of pMad.**Koff-** and **Receptor+** are potential mechanisms on the receptor and BMP:Receptor complex

which eventually lead to promotion of pMad level. Such possible positive feedback loops are predicted in [16].

For each proposed Eiger function, two models were built based on whether Cv2 is exchanging BMP ligands, i.e. whether there are BMP:Cv2:Receptor complexes. Therefore, for three Eiger functions and two Cv2 scenarios, there are 6 combinations. For all the parameters in the model, parameter ranges are selected from previous modeling work and bistability analysis.

4.4 Data Collection

In order to validate each model, data in the form of dorsal view of pMad staining images of different genotypes are collected, and then quantified using Fiji. For each image, a box near the middle of A-P axis is selected, and grayscale data are averaged over A-P direction and thus produce the distribution of fluorescent intensity over D-V axis. To get relative concentration information, the distribution is then calibrated with good quality Wild-Type data from previous work [**?**] and then normalized against Wild-Type distribution maximum value.

In the Result and Discussion section, an example of how a immunofluorescent image data was processed is shown.

4.5 Pareto Frontier

In order to handle different datasets acquired from published literatures of different genotypes, a problem arises as it is hard to compare different models based on multiple potential objectives. A quite possible scenario for so many datasets is that a model performs better for one data set but only if it gets worse for others [57]. In other words, there may be no single best set of parameters for all dataset, instead, there might be a group of parameters shows the compromise or trade-off between fitness of different datasets. Therefore, the current investigation with multiple data sets we have now, the fitness or quantified similarities between model output and one of the

data sets is considered as one objective. An intuitive approach is to sum all objectives and get one single overall fitness or 'sum or error' for all datasets, but this might lead to a problem that some information would be lost since there might be one or more objectives(For example, in this report, datasets with Cv2 and Eiger mutants are more important because these two are the proteins we are interested in). Assigning weights to each objective seems a good idea but the problem is proper weights are yet known just given all datasets in hand. Therefore, a more general method, Pareto Optimization provides an unbiased way for us to compare models we have [58].

A multi-objective optimization serves to find the 'optimal' solution to more than one objective. Pareto optimality, a quite commonly used term in economics when dealing with multi-objective problems, originally means "*a state of allocation of resources in which it is impossible to make any one individual better off without making at least one individual worse off*" [59].

Pareto Optimization is widely used in the area of multiobjective optimization in economics and engineering, but still not a common method in computational biology or bioinformatics. However it has been suggested that it is very promising in tackling many biology related problems like experimental design or protein structure prediction [60]. It can show the trade-off between objectives in a multi-objective problem. For a given problem with more than one objectives, the Pareto frontier is the set of potential states and on this frontier one objective could get better only when the other ones get worse. Finding the Pareto fronts helps us identify potential optimal solutions and have better understanding of the problem by investigating the trade-offs. Figure 4.5 shows a typical 2-objective Pareto frontier, Points P_A and P_B are anchor points, meaning the optimal solution for one objective, and F_u is called 'Utopia' point, meaning the optimal scenario for both objective, and it is usually hard to reach this point. Grey area means feasible region, this is the area in the objective space in which the system can get with the possible parameters. And finally the solid black line shows the Pareto Front, the system can have 'good' solutions on the

front, but when moving on the line, there are trade-offs between two objectives, i.e. if objective A gets better, objective B will definitely get worse.

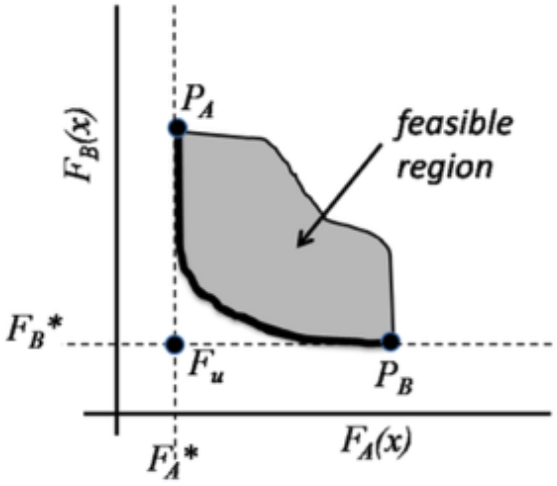

Fig. 4.5. Example of Pareto Front, described in text (Image courtesy of Michael Pargett)

As of comparing different models using Pareto fronts, it is quite obvious that a model would be better if its Pareto front dominates those of the other models.

To calculate the Pareto fronts we used Multi-objective Genetic Algorithm (MOGA) [61], and Normalized Normal Constraints [62]. However, their computational efficiency is not acceptable. In this case, a brute force or Monte Carlo method was used to generate approximate Pareto Fronts. The flowchart of this method used is shown in Figure 4.6.

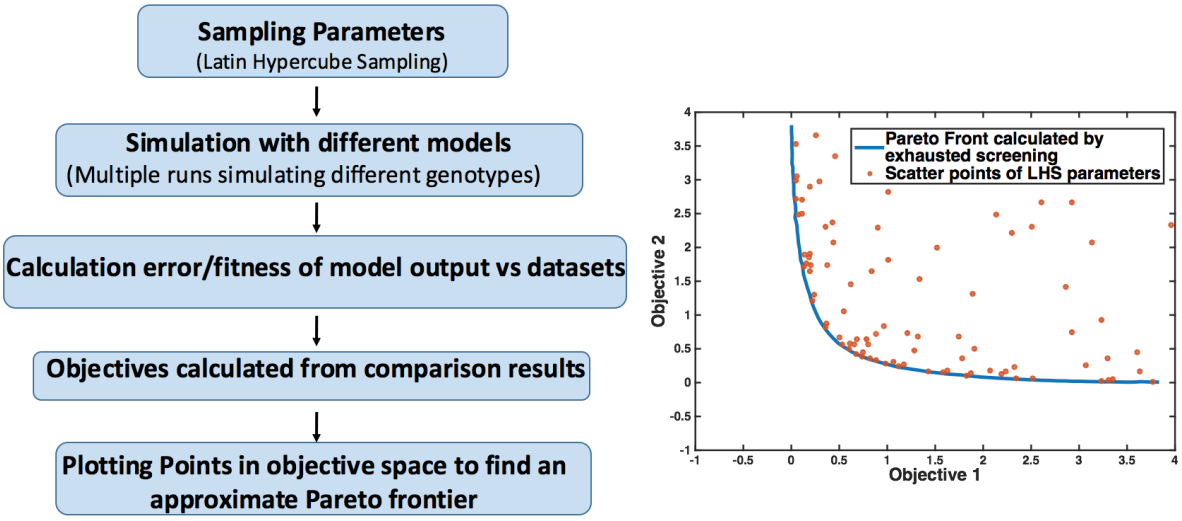

Fig. 4.6. Left: Brute Force Method of generating Pareto Fronts; Right: an example of approximating Pareto frontier for a simple bi-objective problem

5. RESULTS AND DISCUSSION

5.1 Local Model and Bistability Analysis

In order to convert interactions between molecules in the system into mathematical equations, the local model based on the network described in Section 3.1 was built and the ODEs are shown below:

$$\frac{dB}{dt} = \phi_B - k_1 \cdot B \cdot R + k_{-1} \cdot BR - k_2 \cdot B \cdot C + k_{-2} \cdot BC - \delta_B \cdot B$$
$$\frac{dC}{dt} = \frac{\phi_C P^2}{P^2 + K_C^2} - k_2 \cdot B \cdot C + k_{-2} \cdot BC - \delta_C \cdot C$$
$$\frac{dE}{dt} = \frac{\phi_E P^2}{P^2 + K_E^2} - \delta_E \cdot E$$
$$\frac{dBR}{dt} = k_1 \cdot B \cdot R - k_{-1} \cdot BR - \delta_{BR} \cdot BR$$
$$\frac{dBC}{dt} = k_2 \cdot B \cdot C + k_{-2} \cdot BC - \delta_{BC} \cdot BC$$
$$\frac{dP}{dt} = k_s \cdot Mad \cdot BR + k_{se} \cdot Mad \cdot E - k_d \cdot P$$
$$R_{total} = R + BR$$

Let's have a look at the ODEs for Eiger and pMad:

$$\frac{dE}{dt} = \frac{\phi_E P^2}{P^2 + K_E^2} - \delta_E \cdot E$$
$$\frac{dP}{dt} = k_s \cdot Mad \cdot BR + k_{se} \cdot Mad \cdot E - k_d \cdot P$$

By solving at steady-state, we can get:

$$E = \frac{\phi_E P^2}{\delta_E (P^2 + K_E^2)}$$
$$E = \frac{1}{k_{se} \cdot Mad}(k_d \cdot P - k_s \cdot Mad \cdot BR)$$

By plugging the first equation into the second one, we can get:

$$\frac{\phi_E P^2}{\delta_E (P^2 + K_E^2)} = \frac{1}{k_{se} \cdot Mad}(k_d \cdot P - k_s \cdot Mad \cdot BR)$$

By rearranging this equation, we can get a third order polynomial equation like this:

$$k_d P^3 - (k_s \cdot Mad \cdot BR + \frac{k_{se} \cdot Mad \cdot \phi_E}{\delta_E})P^2 + k_d \cdot K_E^2 \cdot P - k_s \cdot Mad \cdot BR \cdot K_E^2 = 0$$

There is another variable BR in the system, but from steady-state equation BR and the relationship between amount of receptors in different form, we have:

$$\frac{dBR}{dt} = k_1 \cdot B \cdot R - k_{-1} \cdot BR - \delta_{BR} \cdot BR$$
$$R_{total} = R + BR$$

Solving these two equation:

$$BR = \frac{k_1 \cdot R_{total} \cdot B}{k_1 \cdot B + k_{-1} + \delta_{BR}}$$

Plug it back in the cubic equation of P:

$$k_d P^3 - (k_s \cdot Mad \cdot \frac{k_1 \cdot R_{total} \cdot B}{k_1 \cdot B + k_{-1} + \delta_{BR}} + \frac{k_{se} \cdot Mad \cdot \phi_E}{\delta_E})P^2 + k_d \cdot K_E^2 \cdot P - k_s \cdot Mad \cdot \frac{k_1 \cdot R_{total} \cdot B}{k_1 \cdot B + k_{-1} + \delta_{BR}} \cdot K_E^2 = 0 \quad (5.1)$$

By solving this cubic equation we can find the steady-state value of P. The number of solutions of this equation depends on parameter values and B, which represent the

extracellular input signal. With proper parameter values, the number of solutions would change with the term B, thus leads to the possibility of ending with multiple steady states, meaning this might be a bistable system.

Based on the cubic equation above, a rough screen over parameters in the equation was run to find a parameter set which ensures the system to have bistability. Bistability analysis was then performed using MatCont. Local model with Cv2 and Eiger showed possibility of having bistability.

For such a parameter set, bifurcation curve showed that with Eiger present in the model, and BMP considered as input signal, pMad as readout, bistability emerges. Curves in Figure 5.1 shows the steady-states 'input' BMP and readout pMad. 'S' shaped curve means that there might be more than one steady states with a same given BMP level. 'LP' stands for limit point, at which the number of steady states would vary. With higher BMP level than the right LP or with lower BMP level than the left LP, the system would only end up on a single steady-state, but when BMP level falls between two LPs, there are more than one steady-states as shown on the curve. For example, a vertical line at BMP level of 0.5 nM would cross the red curve at three different points, this means three steady states. However the middle cross point, the one between two LPs is not 'stable', the system will evolve and move either up to the upper steady states with high pMad readout or go down to the lower steady states with low pMad readout, and this would depend on the dynamic of BMP when this system evolves with time.

Such a system with bistability provides two important features: i) formation of sharp pMad gradient: for low BMP level input, like in cells farther from dorsal midline, the level of pMad would jump to the upper branch if the level of extracellular BMP gets higher the right LP. Once on the upper branch, the level of BR remains there until BMP decreases below the level corresponding to the left LP and leads to the system again back onto the lower branch. This would lead to a 'the rich get richer' situation, in which cells near dorsal midline with initial high level input BMP, would be more competitive than cell away from dorsal midline, especially if amount of BMP

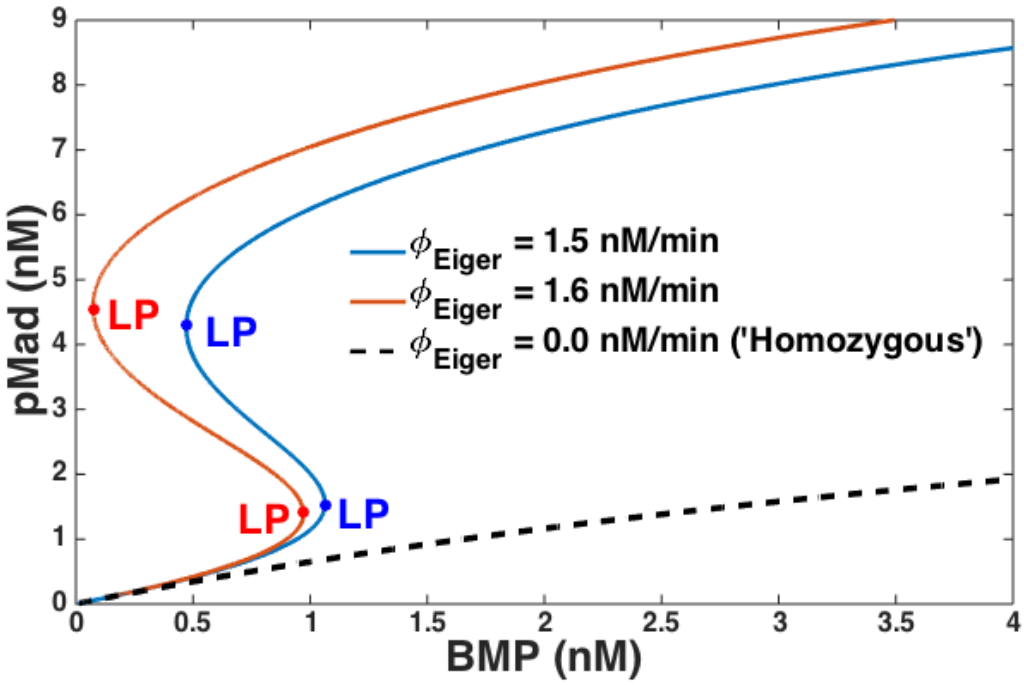

Fig. 5.1. Steady-state Curves of Local Model with different production rate of Eiger

is limited, thus a sharp gradient with high level pMad near dorsal midline and low level away from it. Additionally, the 'jumping' behavior described above results in the sharpness of the distribution. ii) robustness of the system: For a cell, extracellular BMP level might not change gradually as in a smooth curve, potential perturbations from advection or other biochemical processes would cause the input BMP level to be somehow noisy, a bistable system helps improve the robustness by reducing the possible influence on the output (pMad) from the noise of the input (BMP). If BMP fluctuates within the level from left LP to right LP, as stated above, the final pMad state (high or low) would not be affected. It is intuitive to assume that a large such a LP to LP range is more beneficial to the system to tolerate higher noise.

A change of the model, i.e. change of Eiger production level, would affect the stability of the system. As shown in Figure 5.1, with slightly smaller Eiger production rate, the bistability curve is shifted and end up with a smaller LP to LP range. In

another example simulating a heterozygous mutant (production rate of Eiger reduced by half) results in loss of bistability. This means that Eiger plays an important role in gradient formation and provides robustness to the system based on such a bistable system. This can also be found in Equation 5.1 in which Eiger related parameters would be essential to determine number of roots of the polynomial equation. Another information we can get is that without Cv2's intermediating role, meaning the absence of BMP:Cv2:Receptor complex, this equation is not related with Cv2, meaning the bistable system based on Eiger feedback loop is probably not affected by Cv2.

5.2 1D Spatial Model and Bistability

As described above in the Methods section, a one-dimensional spatial model including regional secretion of ligands and diffusion of molecules in the extracellular space is built and simulated to yield the distribution of pMad in space. The transient evolution of pMad signal in different regions in the embryo clearly showed how this bistability system helped a sharp gradient of pMad concentration.

Shown in Figure 5.2, both pMad and BMP gradients evolve with time, but eventually pMad distributions form a much sharper and narrower gradient although the extracellular signal BMP has a rather wider one. Then a closer look at the evolution with time will tell us that extracellular BMP concentrations start with secretion in the dorsal midline range and thus rise to a gradient with its peak at around 10 min, but then the level of BMP would fall. When it reaches steady state, the BMP forms a broad and gradual gradient with relatively low overall concentration. pMad starts with a broad and gradual gradient. Then near the dorsal midline, pMad concentration increases and with a rather fast rate. In the region farther from dorsal midline, pMad rises at first but later falls back to a lower level.

Spatial bistability analysis has been done to show effect of surface BMP-binding protein on BMP:Receptor gradient formation. However if pMad is the signal readout, since most experiments use pMad fluorescent intensity to represent signal level, the

regulation on the level of BMP:Receptor might not be sufficient enough to produce the sharp pMad gradient. This spatial bistability analysis showed the effect of Eiger on the formation of pMad gradient with the positive feedback predicted by Wang and Ferguson [16].

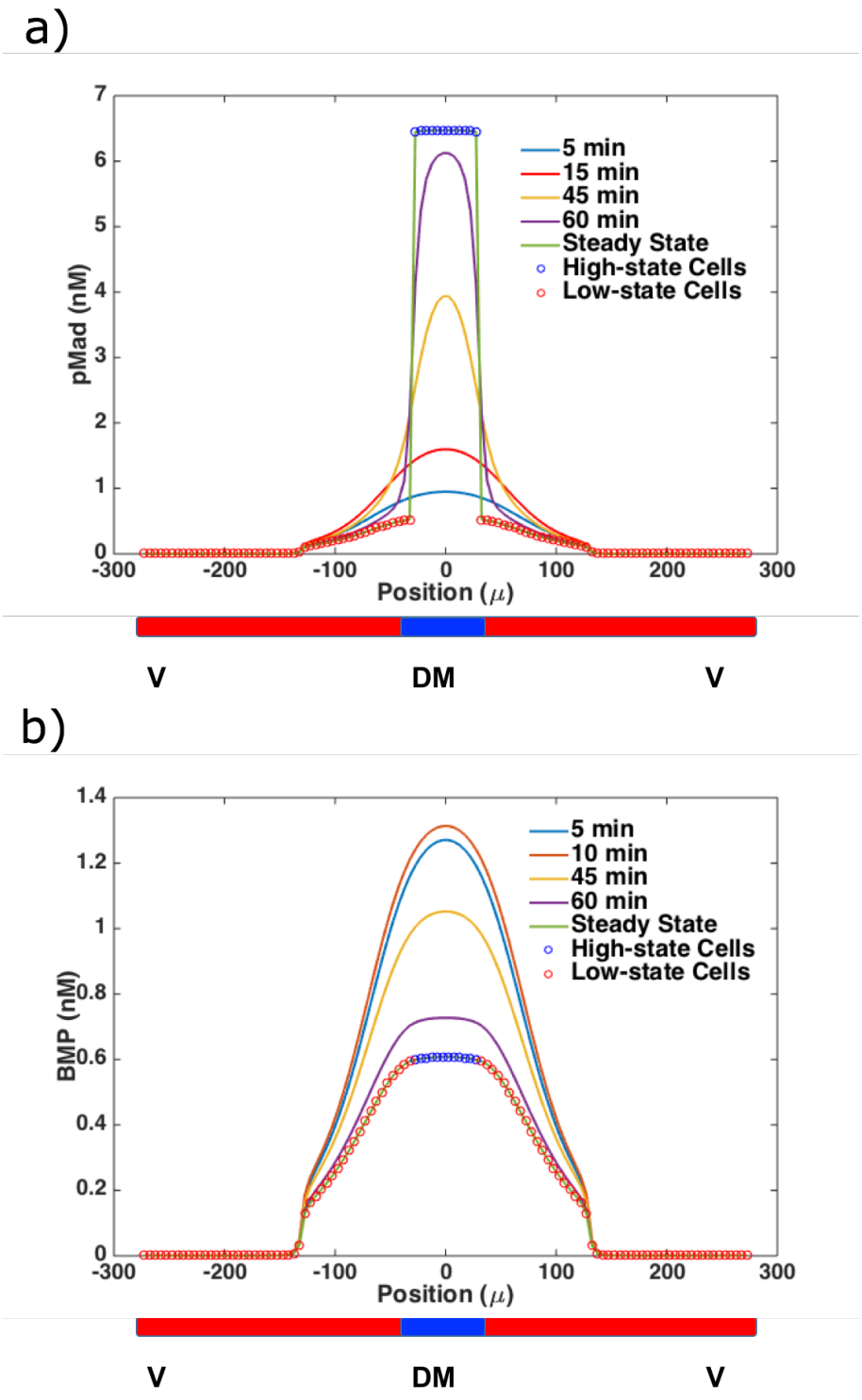

Fig. 5.2. BMP and pMad spatial distribution evolving with time: a) pMad distribution at different time points, circles on the steady state distribution are the pMad levels of cells ending on high or low states of the bistability curve; b) BMP distribution at same time points and cells of high and low pMad states are also showed as circles.

Signal contracts to the dorsal region although the extracellular BMP still have a rather broader distribution. By steady state, cell near dorsal midline stays on high state of the bistatbility curve and farther cells end up on the low state. The dynamics of pMad concentration of two types of cells and how these cells traverse in the states space and finally settle are shown in Figure 5.3. In low-state cells, pMad concentration rises and then falls, the reason can be told in the trace: BMP concentration of these cells rise and fall but the rise doesn't last long to make the system evolve to end up on the high state so it travels back to and settles on the low state.

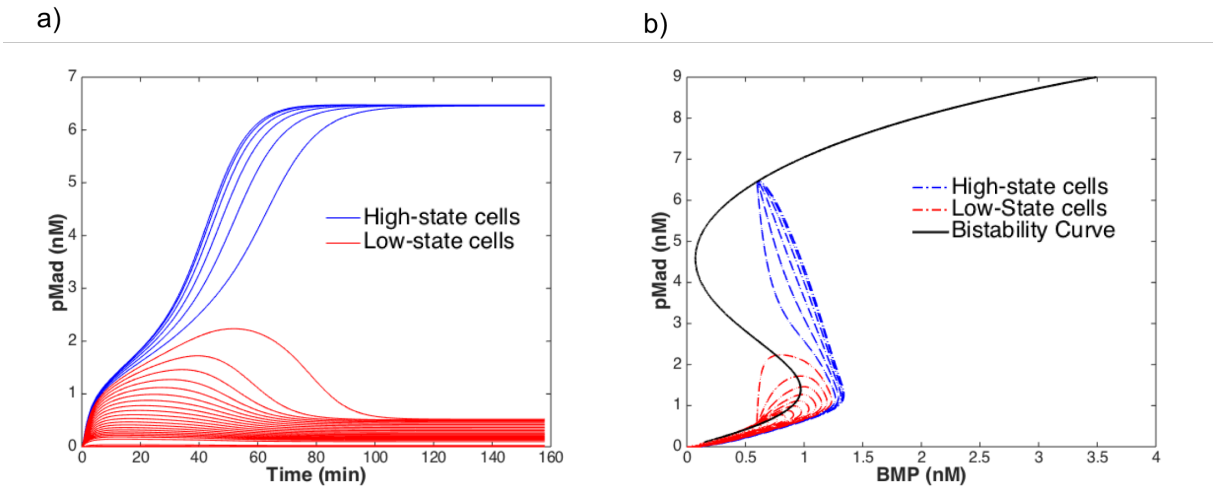

Fig. 5.3. Evolution of pMad ending in two states: a) pMad concentration change with time; b) trace of BMP and pMad concentrations of two types of cells on the stability curve

Such a bistable switch like system helps formation of sharp pMad gradient thus allows cells to know their states more clearly, if we virtually knock down gene *eiger*, as shown in Figure 5.4, the bistability of the system will be lost. Then the final gradient formed is broad and gradual, thus the chance of signal being mis-interpreted is much higher. In conclusion, if Eiger is forming a positive feedback loop in the BMP signal transduction system, it helps formation of a sharp gradient of intracellular signal

readout, pMad. In such way, Eiger might not only help formation of the gradient itself, but also increase the robustness of the cell fates determination process.

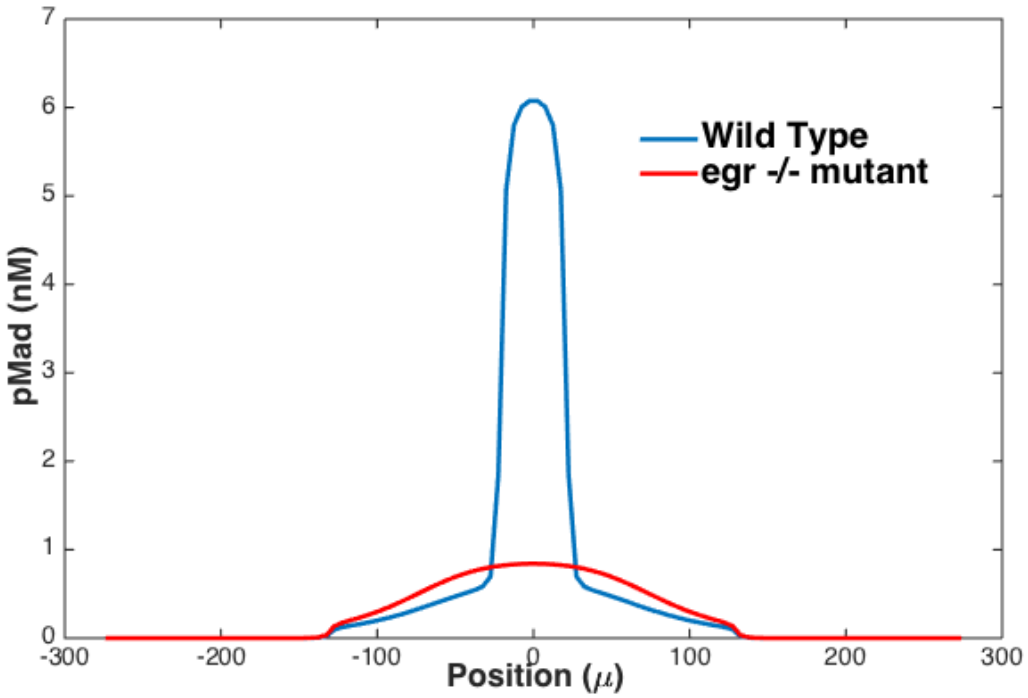

Fig. 5.4. pMad distribution at 60 min of WT and *eiger* heterozygous mutant. In heterozygous simulation, production rate of Eiger is half of the one used in wild type.

5.3 Data Collection and Processing

In order to use experimental data to compare different proposed mechanisms,, pMad staining images of multiple genotypes were collected, working with Thembi Mdluli. The genotypes and data sources are listed below in Table 5.1.

Embryo genotype	**Source**	**Year**
dpp +/-	Wang and Ferguson [16]	2005
tld +/-		
scw -/-		
sog +/-	Peluso et al. [**?**]	2005
sog -/-		
cv2 +/-	Gavin-Smyth et al. [26]	2013
cv2 -/-		
egr -/-		
cv2 , *egr* -/- (double mutant)		
Wild type	Umulis et al. [8]	2010
scw +/-		
sog +/-		

Table 5.1
Table of data used and source

The data are in the format of dorsal view of pMad staining images of embryos. In order to extract data, images are first convert to gray scale image using Image J. Then a box at the middle of the A-P axis with width of 10% of A-P length is drawn, grey scale intensity value is extracted from the area inside the box, and then the data is averaged over the AP axis to get a one-dimensional pMad image intensity distribution along the D-V axis. Since image is taken from dorsal view, it can only cover half of the embryo. The procedure of extracting data from images is shown in Figure 5.5.

In order to get relative concentration information from the gray scale intensity data, a 2 parameter calibration is performed. For a genotype experiment, an image of mutant embryo and a control group wild-type embryo are taken at the same time. Data from both of these images is extracted. From previous work, we have data sets with good quality and well scaled, on concentration and geometry, a reference

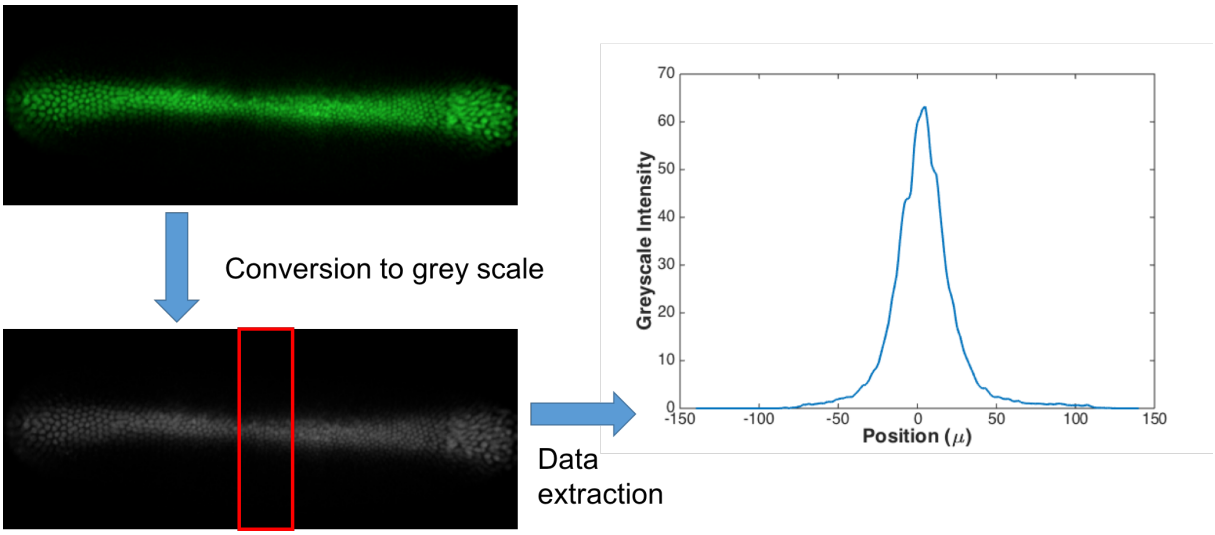

Fig. 5.5. Procedures of data extraction from pMad staining images

wild-type data is adopted from this data set. For a 2 parameter calibration, the relationship of intensity and concentration can be described by equation:

$$Concentration = A \cdot Intensity + B$$

In order to find the two parameter A and B, data at the peak and shoulder of the gradient of both intensity data and reference data are used to solve A and B. Then A and B are used to calibrate the mutant image data. An example of data is shown below in Figure 5.6.

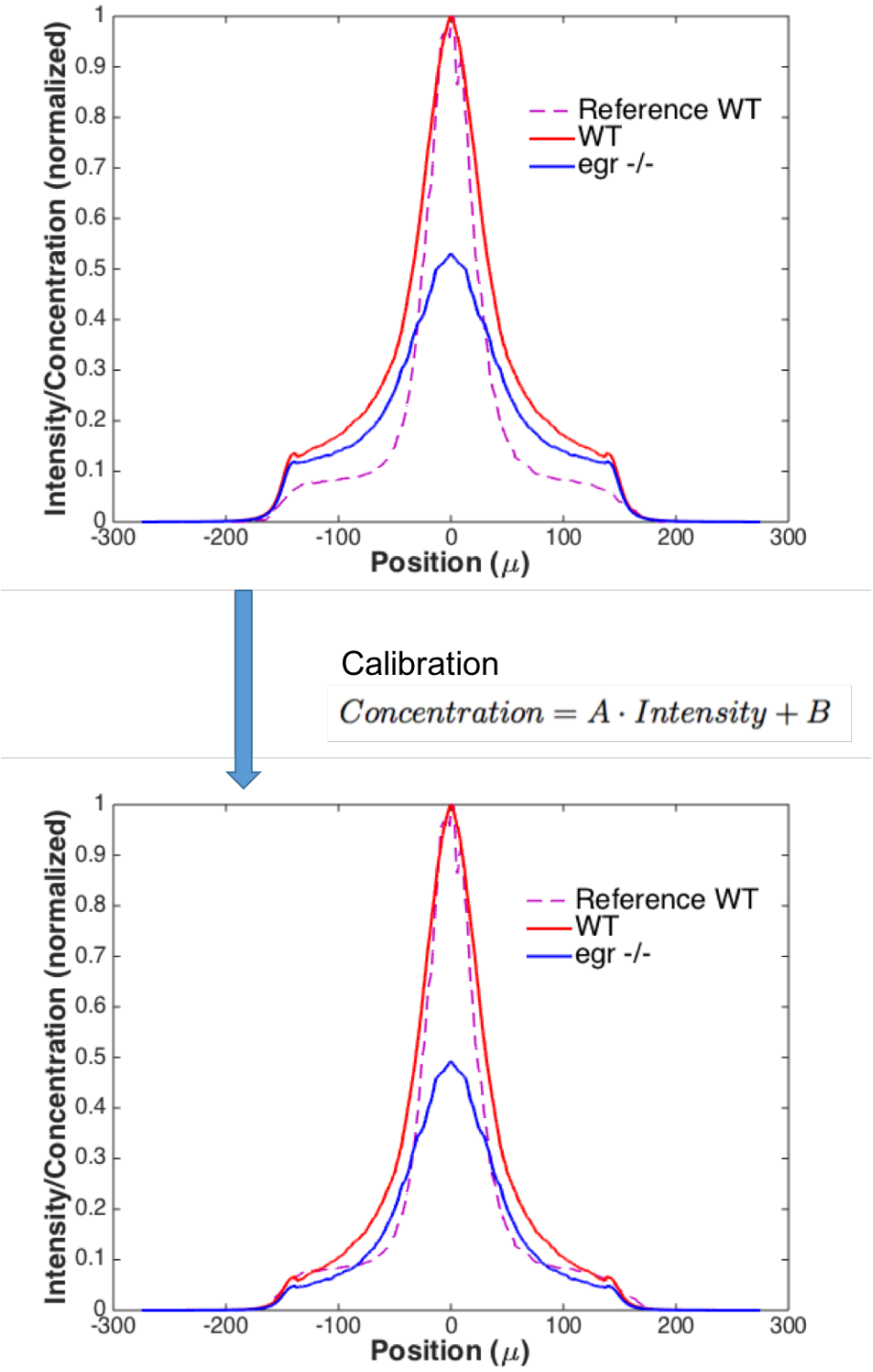

Fig. 5.6. An example (*egr* -/- mutant) of data calibration

5.4 Model Comparison

In order to compare different proposed functions, models are compared by visualizing their Pareto frontiers. The concept of Pareto optimal is described in Section 4.5.

For each parameter set sampled and each one of the models, 12 runs of simulation is done, because the data set used for validation contains 12 different genotypes. Parameter values are modified in order to represent the mutant embryo. For example, in order to simulate *sog* -/- mutant, the production rate of Sog is set to be 0, and for *sog* +/- mutant, the production rate is set to be half of the value used for wild type simulation.

In order to investigate whether the existence of BMP:Cv2:Receptor helps the formation of proper gradient of pMad, a first round of comparison was performed between two models without Eiger and the difference between them is the trimer complex.

To compare model output and data, we calculated the square root of sum of difference between model output concentration and data concentration at 110 points along the D-V axis, because the whole spatial space is discretized into 110 nodes.

$$Comparison(Model \quad vs \quad Data):$$

$$Difference = \sqrt{\sum_{i=1}^{110}(C_i^{model} - C_i^{data})^2}$$

An example of good fitness of simulation results compared to data is shown in Figure 5.7. However, as stated before, such a fit does not necessarily means the model is good because we have multiple data sets, thus multiple objectives. In order to compare different models, Pareto frontiers are calculated. And for better visualization and comparison, mutants are clustered into two major groups, thus forming two major objectives. The first group contains wild type and mutants on genes which produce

extracellular proteins(BMP, Sog/Tsg, Tld) and the second one contains *cv2* mutants, including heterozygous and homozygous mutants.

$$Objective1 = \frac{\sum^{wt+extracellular \quad mutants} Difference}{Number \quad of \quad genotypes}$$

$$Objective1 = \frac{\sum^{cv2 \quad mutants} Difference}{Number \quad of \quad genotypes}$$

The performance of the two models (with or without BCR) is shown in Figure 5.7(b). An important information we can get is that the approximate Pareto frontier of the BCR+ model dominates the one of BCR- model. this means that on both objectives, the BCR+ can reach better optimal.

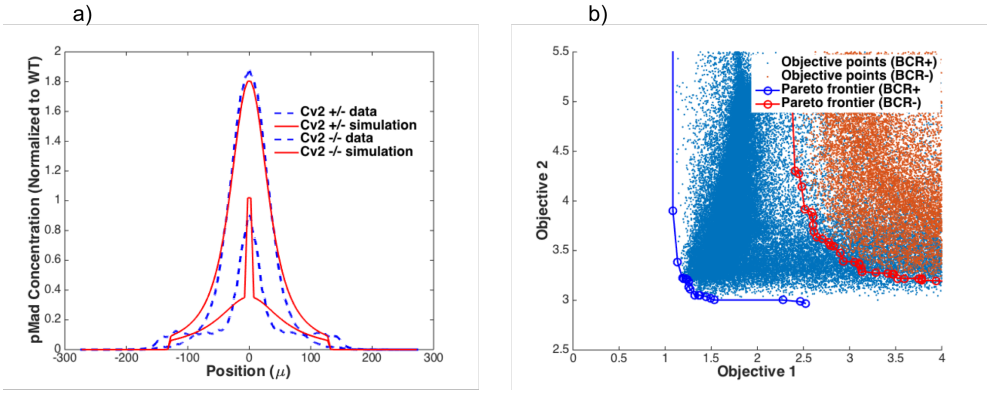

Fig. 5.7. a) An example of simulation result having good fitness of data. b) objective points and Pareto frontier of model BCR+ and BCR-

This shows that the approximation of Pareto fronts works well in comparing different models for such a bi-objective problem. Then, the comparison move on to models including Eiger in the system, as shown in Figure 4.4.

Ks+ Eiger promoting phosphorylation of Mad.

Receptor+ Eiger promoting amount of Receptor.

Koff- Eiger inhibiting dissociation of BMP:Receptor Complex.

For each Eiger function, two models were built based on whether Cv2 is exchanging BMP ligans, i.e. whether there are BMP:Cv2:Receptor complexes. Therefore, for three Eiger functions and two Cv2 scenarios, there are 6 combinations. Objective 1 is *cv2* and *egr* mutants, and Objective 2 is WT and extracellular protein mutants.

First for each Eiger mechanism, a comparison is made for two situation, with or without BCR. The Pareto fronts are shown in Figure 5.8. For all three mechanisms, the comparison is consistent with the result of No Eiger models, which is that BCR improves the optimum of the system Pareto wise.

A strong conclusion can be drawn that the intermediate function of Cv2 is essential in embryonic development in *Drosophila*. It helps the formation of accurate pMad gradient.

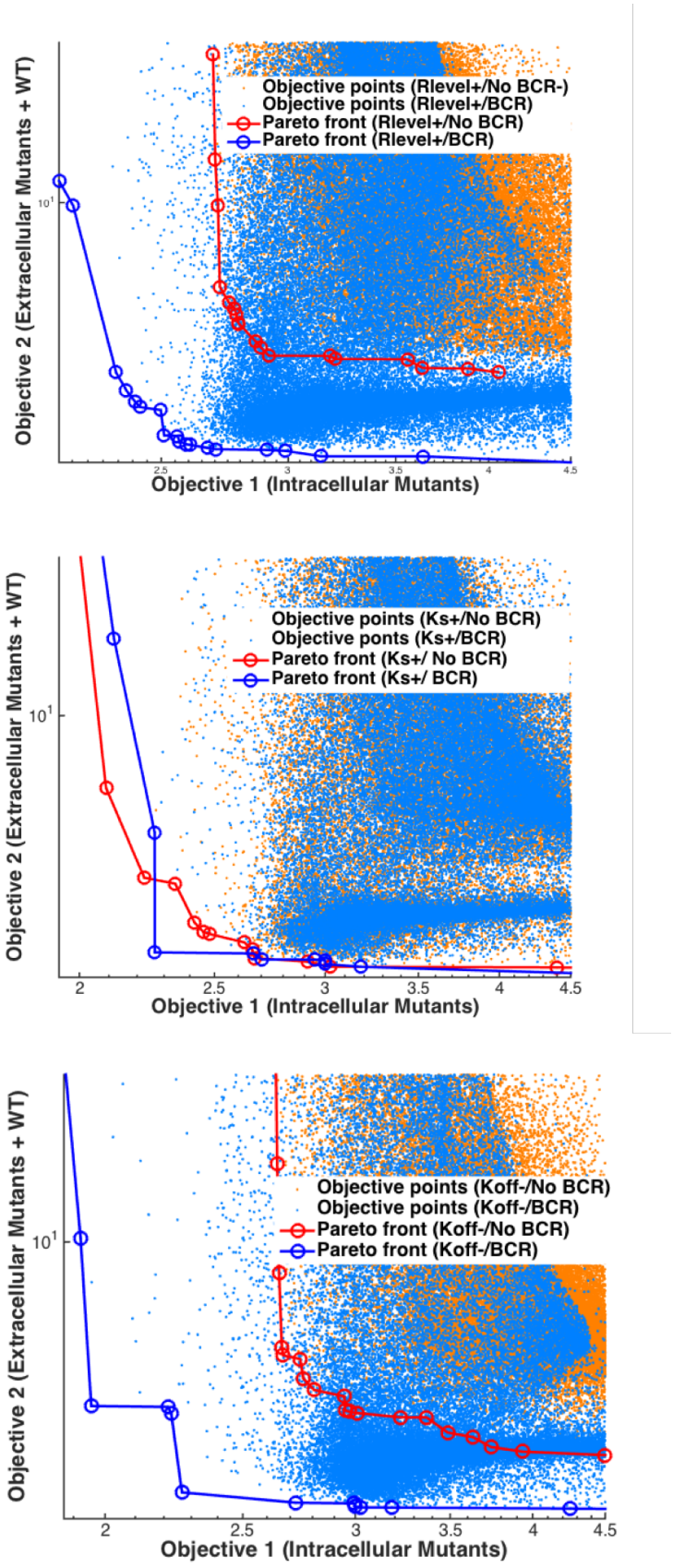

Fig. 5.8. Pareto fronts of models with different Eiger functions and with or without BCR

Then to compare Eiger mechanisms with same Cv2 hypothesis (with BCR), the Pareto fronts of three different models is compared, these three models all include BCR. The Pareto front comparison is shown below in Figure 5.9.

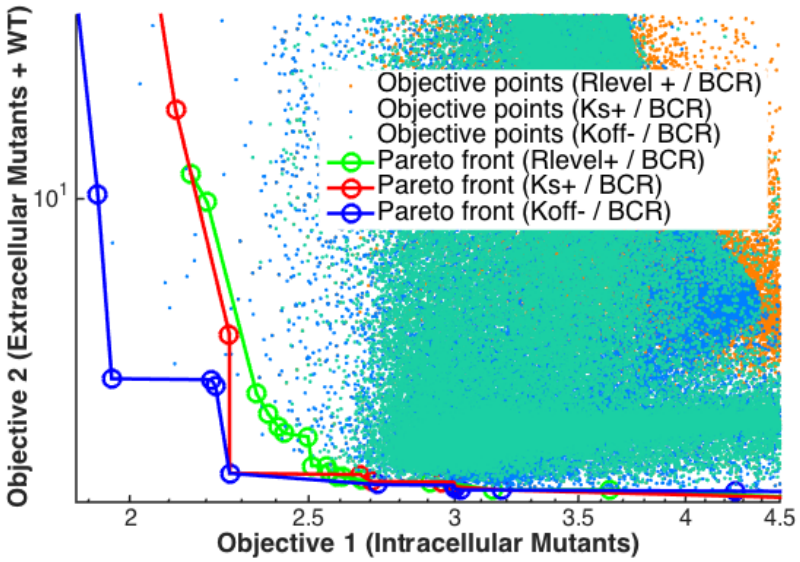

Fig. 5.9. Comparison of different Eiger Function

First, we see Pareto fronts that on Objective 2, which represents the models' performance on WT and mutants on extracellular proteins, all three models perform quite well. This is because the extracellular shuttling system is not directly linked with function of Eiger. Secondly, on Objective 2, which should be more informative when comparing Eiger functions, the Koff- model works better, the Pareto front of it dominates those of the other model. This means it is more possible that Eiger's biological function is to mediate the kinetics of BMP and receptors binding. Eiger's homolog, TNF-alpha protein was found to be a transmembrane protein, so Eiger can also be a protein on membrane and then interact with BMP or receptor so that the dissociation of BMP:Receptor complex is down regulated by it, thus providing feedback loop to the system. Previous model predicted possible feedback on receptors [49], this feedback can be conducted by Eiger in such a mechanism.

From the models tested above, a current conclusion of this report can be stated from comparing different mechanisms proposed: i) Cv2's intermediating function is essential in *Drosophila* embryo, supporting the hypothesis where the BMP:Cv2:Receptor complex exists; ii) Eiger is a protein up regulated by pMad and it can in turn act on the BMP signal transduction by inhibiting the dissociation of BMP:Receptor complex.

6. CONCLUSION AND FUTURE WORK

From the mathematic modeling work done in this project, the functions of Eiger and Cv2 in the BMP-mediated morphogenesis are investigated. Some conclusion can be drawn:

Feedback and Bistability Analysis Eiger is promoted by pMad, the intracellular messenger of BMP signal, and Eiger can in turn promote pMad level. This positive feedback can lead to non-linearty in the system and thus lead to a bistable switch like behavior. As shown in the bistability analysis on a local model representing a single cell and a spatial model representing D-V axis, such a system with positive feedback improves the likelihood of formation of a sharp pMad gradient and resembles the experimental findings. Bistability analysis on both local and spatial domains demonstrated such benefits: i) Although BMP forms a gradual gradient, the intracellular messenger still ends up with a sharp gradient because of the bistability; ii) Eiger plays a key role in the formation of the gradient, a slight perturbation of Eiger would cause the system to loose bistability such that the sharp gradient no longer exists, this is also predicted by simulation of Eiger mutant embryo which agreed with experimental results qualitatively. Another important finding of positive feedback with Eiger is that the level of signaling is determined by how the extracellular BMP level evolve with time at different locations.

Pareto front for Comparing Mechanisms Modeling of biological contexts like a system of BMP signaling would require fitting of multiple data sets at the same time.A direct approach is to use these data sets, in this case, pMad concentration gradient of different genotypes, to train and validate models However this may be difficult to find a single parameter set which satisfies all require-

ments. Therefore, multi-objective optimization (MOO) is a useful technique to take all objectives and all data sets into consideration, which has already been shown to be better than single-objective approaches in many cases, and more importantly MOO is a potentially useful tool in computational biology and bioinformatics [60]. Pareto optimality is one widely used concept in MOO, it showed the trade off between objectives in a system. By constructing a Pareto frontier, models can be compared by their simultaneous performance on more than one objectives. Multiple objectives are constructed from data of different genotypes. In this project Pareto front works as a good mathematical tool to find the optimal or quasi-optimal situation for such a problem. Clear trade-off between objectives are shown, this might be helpful for further analysis. Different models based on different potential mechanisms, were built and a bi-objective Pareto front of each model was used to compare them. These Pereto fronts showed clear trade-off between objectives and clearly distinguished these models by their performance on both objectives. An optimal mechanism, with Eiger inhibiting BMP:Receptor dissociation and Cv2 intermediating BMP by forming BMP:Cv2:Receptor complex was identified.

Cv2 intermediating BMP and Receptor binding By comparing different mechanisms, it is found that the presence of BCR leads to better models. So in *Drosophila* embryo, it is more likely that Cv2 is intermediating BMP and receptor kinetics by forming a trimer complex BMP:Cv2:Receptor. This trimer complex was studied computationally and experimentally on *Drosophila* wing discs and it was found to have a biphasic function on BMP signaling, however in *Drosophila* embryo, formation of such a trimer with Cv2 up-regulated by pMad is never confirmed. Pareto fronts comparison in this work clearly showed that the system with BCR complex is better on both objectives compared with the one without it. So we predict that in *Drosophila* embryo, Cv2 is also intermediating BMP on membrane and thus forming a rather complicated feedback loop which may also have a biphasic effect.

Eiger preventing BMP:Receptor dissociation Eiger is a homolog of TNF-alpha protein which is an essential part in JNK pathway in Drosophila. Study on Eiger is limited compared to Cv2, especially in details of functioning mechanisms. Experimental results showed that Eiger is downstream target gene of pMad and in the mean time it is promoting pMad signal. In the Pareto front comparison, we tested three different Eiger potential mechanisms. It showed that Eiger is potentially down regulating BMP:Receptor dissociation thus promoting pMad generation. This would close the feedback loop in the system. Such a system with BMP:Receptor dissociation inhibited had better performance on the objective which is constructed by Cv2 and Eiger mutants. This would suggest that among the mechanisms proposed, Eiger is more likely to show effects on BR complex. Study on TNF-alpha protein family showed that it can be cross-membrane protein, so maybe Eiger is also intermediating interactions between BMP and cross-membrane receptors. Or indirectly, Eiger is affecting this system via JNK pathway. With our prediction from the best model being composed of Eiger inhibiting BMP:Receptor dissociation, more experimental and computational work could be done to deny it or find biochemical proof of it.

Exploiting the intracellular regulators' characteristics in BMP signal network does not only answers some unanswered questions, but also helps us find solutions to biomedical problems. For example, with Eiger's function unveiled, the ability of controlling embryonic stem cell differentiation in stem cell therapy might be possible.

This study investigates with models that Eiger may play roles in BMP signal transduction, but other studies also found Eiger is an important part in damage-induced neuronal apoptosis [52]. Still other have found that, as a fat-body derived signal released in the hemolymph in response to starvation, Eiger is an adipokine that reduces the expression of insulin-like peptides by remotely acting on its receptor Grindelwald locally expressed in the brain insulin-producing cells [53]. As a part in multiple import pathways, there might be some crosstalsk between BMP network and others linked by Eiger. Experimental study like investing neuronal apoptosis when

perturbating BMP can be done to test this hypothesis. Mathematical model can also be adopted to study the cross-talk between different pathways: i) effect from other pathways can be introduced by adding components to the present network, like the research [48] on Gurken pathway and BMP signaling; ii) integration of different pathways can be studied by logical modeling or boolean models in which gene regulatory networks are abstracted and data in other forms can be incorporated.

To test the prediction made in this report, *in vitro* experiment can be done by examining the kinetics of interaction between BMP and receptor with or without Eiger. *in vivo* experiments can be designed by model based experimental design. Starting from the model selected by this work, *in silico* perturbation can be easily performed on more than one genes, these simulating experiments would return a collection of results and among them we can find the most informative one. Double mutants experiment is ideal for model based experimental design because simulation can easily find the best or the most informative combination of genes to knock down.

With mathematical modeling and experimental research combined, the understanding of Eiger and Cv2 in BMP signaling, or even a much bigger picture, will be improved, leading to deciphering secrets BMP governed patterning and improved treatment of BMP-related developmental disorder.

LIST OF REFERENCES

LIST OF REFERENCES

[1] P. Ball, P. Ball, P. Ball, and P. Ball, *Nature's patterns: a tapestry in three parts*. Oxford ; New York: Oxford University Press, 2011.

[2] M. J. Tyler and D. A. Cameron, "Cellular pattern formation during retinal regeneration: A role for homotypic control of cell fate acquisition," *Vision Research*, vol. 47, pp. 501–511, Feb. 2007.

[3] A. D. Lander, Q. Nie, and F. Y. Wan, "Do Morphogen Gradients Arise by Diffusion?," *Developmental Cell*, vol. 2, pp. 785–796, June 2002.

[4] A. M. Turing, "The Chemical Basis of Morphogenesis," *Philosophical Transactions of the Royal Society B: Biological Sciences*, vol. 237, pp. 37–72, Aug. 1952.

[5] J. B. Gurdon and P.-Y. Bourillot, "Morphogen gradient interpretation," *Nature*, vol. 413, no. 6858, pp. 797–803, 2001.

[6] H. L. Ashe, "The interpretation of morphogen gradients," *Development*, vol. 133, pp. 385–394, Feb. 2006.

[7] S. A. Bleuming, X. C. He, L. L. Kodach, J. C. Hardwick, F. A. Koopman, F. J. ten Kate, S. J. van Deventer, D. W. Hommes, M. P. Peppelenbosch, G. J. Offerhaus, L. Li, and G. R. van den Brink, "Bone Morphogenetic Protein Signaling Suppresses Tumorigenesis at Gastric Epithelial Transition Zones in Mice," *Cancer Research*, vol. 67, pp. 8149–8155, Sept. 2007.

[8] D. M. Umulis, O. Shimmi, M. B. O'Connor, and H. G. Othmer, "Organism-scale modeling of early Drosophila patterning via bone morphogenetic proteins," *Developmental Cell*, vol. 18, pp. 260–274, Feb. 2010.

[9] S. C. Little and M. C. Mullins, "Bone morphogenetic protein heterodimers assemble heteromeric type I receptor complexes to pattern the dorsoventral axis," *Nature Cell Biology*, vol. 11, pp. 637–643, May 2009.

[10] M. D. Adams and *et al.*, "The genome sequence of Drosophila melanogaster," *Science (New York, N.Y.)*, vol. 287, pp. 2185–2195, Mar. 2000.

[11] L. T. Reiter, "A Systematic Analysis of Human Disease-Associated Gene Sequences In Drosophila melanogaster," *Genome Research*, vol. 11, pp. 1114–1125, June 2001.

[12] R. W. Padgett, J. M. Wozney, and W. M. Gelbart, "Human BMP sequences can confer normal dorsal-ventral patterning in the Drosophila embryo," *Proceedings of the National Academy of Sciences of the United States of America*, vol. 90, pp. 2905–2909, Apr. 1993.

[13] L. Wolpert, "Positional information and the spatial pattern of cellular differentiation," *Journal of Theoretical Biology*, vol. 25, pp. 1–47, Oct. 1969.

[14] W. Driever and C. Nüsslein-Volhard, "The bicoid protein determines position in the Drosophila embryo in a concentration-dependent manner," *Cell*, vol. 54, pp. 95–104, July 1988.

[15] D. J. Sutherland, "Stepwise formation of a SMAD activity gradient during dorsal-ventral patterning of the Drosophila embryo," *Development*, vol. 130, pp. 5705–5716, Dec. 2003.

[16] Y.-C. Wang and E. L. Ferguson, "Spatial bistability of Dpp–receptor interactions during Drosophila dorsal–ventral patterning," *Nature*, vol. 434, pp. 229–234, Mar. 2005.

[17] M. B. O'Connor, "Shaping BMP morphogen gradients in the Drosophila embryo and pupal wing," *Development*, vol. 133, pp. 183–193, Dec. 2005.

[18] B. Biehs, V. François, and E. Bier, "The Drosophila short gastrulation gene prevents Dpp from autoactivating and suppressing neurogenesis in the neuroectoderm," *Genes & Development*, vol. 10, pp. 2922–2934, Nov. 1996.

[19] C. Chang, D. A. Holtzman, S. Chau, T. Chickering, E. A. Woolf, L. M. Holmgren, J. Bodorova, D. P. Gearing, W. E. Holmes, and A. H. Brivanlou, "Twisted gastrulation can function as a BMP antagonist," *Nature*, vol. 410, pp. 483–487, Mar. 2001.

[20] O. Shimmi, D. Umulis, H. Othmer, and M. B. O'Connor, "Facilitated transport of a Dpp/Scw heterodimer by Sog/Tsg leads to robust patterning of the Drosophila blastoderm embryo," *Cell*, vol. 120, pp. 873–886, Mar. 2005.

[21] D. Umulis, M. B. O'Connor, and H. G. Othmer, "Robustness of Embryonic Spatial Patterning in Drosophila melanogaster," in *Current Topics in Developmental Biology*, vol. 81, pp. 65–111, Elsevier, 2008.

[22] D. Umulis, M. B. O'Connor, and S. S. Blair, "The extracellular regulation of bone morphogenetic protein signaling," *Development*, vol. 136, pp. 3715–3728, Nov. 2009.

[23] H.-W. Kang, L. Zheng, and H. G. Othmer, "The effect of the signalling scheme on the robustness of pattern formation in development," *Interface Focus*, vol. 2, pp. 465–486, Aug. 2012.

[24] D. M. Umulis, M. Serpe, M. B. O'Connor, and H. G. Othmer, "Robust, bistable patterning of the dorsal surface of the Drosophila embryo," *Proceedings of the National Academy of Sciences*, vol. 103, pp. 11613–11618, Aug. 2006.

[25] M. S. Karim, G. T. Buzzard, and D. M. Umulis, "Secreted, receptor-associated bone morphogenetic protein regulators reduce stochastic noise intrinsic to many extracellular morphogen distributions," *Journal of The Royal Society Interface*, vol. 9, pp. 1073–1083, May 2012.

[26] J. Gavin-Smyth, Y.-C. Wang, I. Butler, and E. L. Ferguson, "A Genetic Network Conferring Canalization to a Bistable Patterning System in Drosophila," *Current Biology*, vol. 23, pp. 2296–2302, Nov. 2013.

[27] S. Saremba, J. Nickel, A. Seher, A. Kotzsch, W. Sebald, and T. D. Mueller, "Type I receptor binding of bone morphogenetic protein 6 is dependent on N-glycosylation of the ligand: Type I receptor specificity of BMP-6," *FEBS Journal*, vol. 275, pp. 172–183, Jan. 2008.

[28] F. Rentzsch, "Crossveinless 2 is an essential positive feedback regulator of Bmp signaling during zebrafish gastrulation," *Development*, vol. 133, pp. 801–811, Mar. 2006.

[29] L. Wolpert, ed., *Principles of development*. Oxford ; New York: Oxford University Press, 4th ed ed., 2011.

[30] A. Martinez Arias and A. Stewart, *Molecular principles of animal development*. Oxford ; New York: Oxford University Press, 2002.

[31] A. Gierer and H. Meinhardt, "A theory of biological pattern formation," *Kybernetik*, vol. 12, pp. 30–39, Dec. 1972.

[32] J. B. A. Green and J. Sharpe, "Positional information and reaction-diffusion: two big ideas in developmental biology combine," *Development*, vol. 142, pp. 1203–1211, Apr. 2015.

[33] J. Raspopovic, L. Marcon, L. Russo, and J. Sharpe, "Digit patterning is controlled by a Bmp-Sox9-Wnt Turing network modulated by morphogen gradients," *Science*, vol. 345, pp. 566–570, Aug. 2014.

[34] Z. Feng, W. Zhang, J. Xu, C. Gauron, B. Ducos, S. Vriz, M. Volovitch, L. Jullien, S. Weiss, and D. Bensimon, "Optical control and study of biological processes at the single-cell level in a live organism," *Reports on Progress in Physics*, vol. 76, p. 072601, July 2013.

[35] E. L. Ferguson and K. V. Anderson, "Decapentaplegic acts as a morphogen to organize dorsal-ventral pattern in the Drosophila embryo," *Cell*, vol. 71, pp. 451–461, Oct. 1992.

[36] H. L. Ashe, M. Mannervik, and M. Levine, "Dpp signaling thresholds in the dorsal ectoderm of the Drosophila embryo," *Development (Cambridge, England)*, vol. 127, pp. 3305–3312, Aug. 2000.

[37] M. Affolter and K. Basler, "The Decapentaplegic morphogen gradient: from pattern formation to growth regulation," *Nature Reviews Genetics*, vol. 8, pp. 663–674, Sept. 2007.

[38] A. H. Reddi and A. Reddi, "Bone morphogenetic proteins (BMPs): From morphogens to metabologens," *Cytokine & Growth Factor Reviews*, vol. 20, pp. 341–342, Oct. 2009.

[39] E. Ruberte, T. Marty, D. Nellen, M. Affolter, and K. Basler, "An absolute requirement for both the type II and type I receptors, punt and thick veins, for Dpp signaling in vivo," *Cell*, vol. 80, pp. 889–897, Mar. 1995.

[40] B. Schmierer, A. L. Tournier, P. A. Bates, and C. S. Hill, "Mathematical modeling identifies Smad nucleocytoplasmic shuttling as a dynamic signal-interpreting system," *Proceedings of the National Academy of Sciences*, vol. 105, pp. 6608–6613, May 2008.

[41] H. L. Ashe and M. Levine, "Local inhibition and long-range enhancement of Dpp signal transduction by Sog," *Nature*, vol. 398, pp. 427–431, Apr. 1999.

[42] J. Künnapuu, P. M. Tauscher, N. Tiusanen, M. Nguyen, A. Löytynoja, K. Arora, and O. Shimmi, "Cleavage of the Drosophila screw prodomain is critical for a dynamic BMP morphogen gradient in embryogenesis," *Developmental Biology*, vol. 389, pp. 149–159, May 2014.

[43] J. Winstanley, A. Sawala, C. Baldock, and H. L. Ashe, "Synthetic enzyme-substrate tethering obviates the Tolloid-ECM interaction during *drosophila* BMP gradient formation," *eLife*, vol. 4, Feb. 2015.

[44] E. Bier and E. M. De Robertis, "BMP gradients: A paradigm for morphogen-mediated developmental patterning," *Science*, vol. 348, pp. aaa5838–aaa5838, June 2015.

[45] A. Eldar, R. Dorfman, D. Weiss, H. Ashe, B.-Z. Shilo, and N. Barkai, "Robustness of the BMP morphogen gradient in Drosophila embryonic patterning," *Nature*, vol. 419, pp. 304–308, Sept. 2002.

[46] Y. Lou, Q. Nie, and F. Y. M. Wan, "Effects of Sog on Dpp-Receptor Binding," *SIAM Journal on Applied Mathematics*, vol. 65, pp. 1748–1771, Jan. 2005.

[47] P. Muller, K. W. Rogers, S. R. Yu, M. Brand, and A. F. Schier, "Morphogen transport," *Development*, vol. 140, pp. 1621–1638, Apr. 2013.

[48] J. Lembong, N. Yakoby, and S. Y. Shvartsman, "Pattern formation by dynamically interacting network motifs," *Proceedings of the National Academy of Sciences*, vol. 106, pp. 3213–3218, Mar. 2009.

[49] M. G. Niepielko, K. Ip, J. S. Kanodia, D. S. Lun, and N. Yakoby, "Evolution of BMP Signaling in Drosophila Oogenesis: A Receptor-Based Mechanism," *Biophysical Journal*, vol. 102, pp. 1722–1730, Apr. 2012.

[50] A. L. Ambrosio, V. F. Taelman, H. X. Lee, C. A. Metzinger, C. Coffinier, and E. De Robertis, "Crossveinless-2 Is a BMP Feedback Inhibitor that Binds Chordin/BMP to Regulate Xenopus Embryonic Patterning," *Developmental Cell*, vol. 15, pp. 248–260, Aug. 2008.

[51] J.-l. Zhang, L.-y. Qiu, A. Kotzsch, S. Weidauer, L. Patterson, M. Hammerschmidt, W. Sebald, and T. D. Mueller, "Crystal Structure Analysis Reveals How the Chordin Family Member Crossveinless 2 Blocks BMP-2 Receptor Binding," *Developmental Cell*, vol. 14, pp. 739–750, May 2008.

[52] J. Shklover, F. Levy-Adam, and E. Kurant, "The role of *drosophila* TNF Eiger in developmental and damage-induced neuronal apoptosis," *FEBS Letters*, vol. 589, pp. 871–879, Apr. 2015.

[53] N. Agrawal, R. Delanoue, A. Mauri, D. Basco, M. Pasco, B. Thorens, and P. Léopold, "The Drosophila TNF Eiger Is an Adipokine that Acts on Insulin-Producing Cells to Mediate Nutrient Response," *Cell Metabolism*, vol. 23, pp. 675–684, Apr. 2016.

[54] L. F. Shampine and M. W. Reichelt, "The MATLAB ODE Suite," *SIAM Journal on Scientific Computing*, vol. 18, pp. 1–22, Jan. 1997.

[55] L. F. Shampine, M. W. Reichelt, and J. A. Kierzenka, "Solving Index-1 DAEs in MATLAB and Simulink," *SIAM Review*, vol. 41, pp. 538–552, Jan. 1999.

[56] W. Govaerts, Y. Kuznetsov, and B. Sautois, "MATCONT," *Scholarpedia*, vol. 1, no. 9, p. 1375, 2006.

[57] M. Pargett and D. M. Umulis, "Quantitative model analysis with diverse biological data: Applications in developmental pattern formation," *Methods*, vol. 62, pp. 56–67, July 2013.

[58] P. Ngatchou, A. Zarei, and A. El-Sharkawi, "Pareto Multi Objective Optimization," pp. 84–91, IEEE, 2005.

[59] N. A. Barr, *The economics of the welfare state*. Oxford ; New York: Oxford University Press, 5th ed ed., 2012.

[60] J. Handl, D. B. Kell, and J. Knowles, "Multiobjective Optimization in Bioinformatics and Computational Biology," *IEEE/ACM Transactions on Computational Biology and Bioinformatics*, vol. 4, pp. 279–292, Apr. 2007.

[61] Institute of Electrical and Electronics Engineers, ed., *1995 IEEE International Conference on Evolutionary Computation, the University of Western Australia, Perth, Western Australia, 29 November-1 December, 1995*. [New York] : Piscataway, NJ: Institute of Electrical and Electronics Engineers ; Available from IEEE Service Center, 1995.

[62] A. Messac, A. Ismail-Yahaya, and C. Mattson, "The normalized normal constraint method for generating the Pareto frontier," *Structural and Multidisciplinary Optimization*, vol. 25, pp. 86–98, July 2003.